

MICROCOPY RESOLUTION TEST CHART
NATIONAL BUREAU OF STANDARDS-1963-A

AFOSR TR. 3 11 82

2

ADA 162 747 ✓

September 10, 1985

Annual Scientific Report for Grant No. AFOSR-82-0314
Covering the Period from 1 August 1984 to 31 July 1985

ELECTRON PRODUCTION, ELECTRON ATTACHMENT, AND CHARGE
RECOMBINATION PROCESS IN HIGH PRESSURE GAS DISCHARGES

By: Long C. Lee
Department of Electrical and Computer Engineering
San Diego State University
San Diego, California 92182-0190
Telephone: (619) 265-3701

DTIC
ELECTE
S DEC 30 1985 D

Prepared for:

U. S. Air Force Office of Scientific Research
Bolling Air Force Base
Washington, D. C. 20332-6448
Attention: Major Bruce L. Smith
Directorate of Physical and Geophysical
Sciences

DTIC FILE COPY

DISTRIBUTION STATEMENT A
Approved for public release;
Distribution Unlimited

AD-A162 747

UNCLASSIFIED

SECURITY CLASSIFICATION OF THIS PAGE (When Data Entered)

REPORT DOCUMENTATION PAGE		READ INSTRUCTIONS BEFORE COMPLETING FORM
1. REPORT NUMBER AFOSR-TR- 85-1132	2. GOVT ACCESSION NO. AD-A162 747	3. REPORT'S CATALOG NUMBER
4. TITLE (and Subtitle) Electron Production, Electron Attachment, and Charge Recombination Process in High Pressure Gas Discharges		5. TYPE OF REPORT & PERIOD COVERED Annual Report 1 August 1984 - 31 July 1985
7. AUTHOR(s) Long C. Lee		6. PERFORMING ORG. REPORT NUMBER
9. PERFORMING ORGANIZATION NAME AND ADDRESS San Diego State University San Diego, California 92182		8. CONTRACT OR GRANT NUMBER(s) AFOSR-82-0314
11. CONTROLLING OFFICE NAME AND ADDRESS U. S. Air Force of Scientific Research Bolling Air Force Base Washington, D.C. 20332		10. PROGRAM ELEMENT, PROJECT, TASK AREA & WORK UNIT NUMBERS 61102F 2301/A7
14. MONITORING AGENCY NAME & ADDRESS (if different from Controlling Office)		12. REPORT DATE 10 September 1985
		13. NUMBER OF PAGES 31
		15. SECURITY CLASS. (of this report) Unclassified
		15a. DECLASSIFICATION DOWNGRADING SCHEDULE
16. DISTRIBUTION STATEMENT (of this Report) Approved for public release; distribution unlimited		
17. DISTRIBUTION STATEMENT (of the abstract entered in Block 20, if different from Report)		
18. SUPPLEMENTARY NOTES The findings in this report are not to be constructed as an official position of the Department of the Air Force, unless so designated by other authorized documents.		
19. KEY WORDS (Continue on reverse side if necessary and identify by block number) Electron production; electron attachment; electron diffusion; charge recombination; electron conduction current; temporary negative ion; space charge effect; plasma decay; electron leakage from plasma; electron attaching gas; excimer laser; parallel-plate drift-tube apparatus; computer modeling		
20. ABSTRACT (Continue on reverse side if necessary and identify by block number) The electron productions from two-photon-ionization of CS₂, SO₂ and (CH₃)₃N at 193 nm were investigated and their coefficients were measured. The effect of space charge on the electron conduction pulse was observed as a function of charge density and the applied electric field. The electron attachment rate constants of H₂O and C₃F₈ in buffer gases of Ar, N₂, and CH₄ were measured. The electron attachment rate constants for the gas mixtures of H₂O-Ar, C₃F₈-N₂ and C₃F₈-CH₄ increase with increasing E/N. These characteristics are useful for the application of opening switches. The electron drift velocities of various gas mixtures were measured.		

I. INTRODUCTION

This annual report covers the period from August 1, 1984 to July 31, 1985 for the research project under Grant No. AFOSR-82-0314. In this research program, the processes for electron production, electron attachment and charge recombination in high pressure gaseous mixtures were investigated. The information obtained from this research is currently needed for developing various electrical switching devices as well as for understanding the basic phenomena in plasma physics.

Various electrical switching devices, such as high energy and high repetition-rate discharge switches, opening switches, radiation or e-beam controlled switches, are needed for the development of high power lasers, fusion experiment, magnetic energy storage system, as well as particle beam experiment. High pressure gaseous discharges are frequently used in these switching devices. For a specific discharge switch, it may require some special characteristics pertinent to the pulse rise and decay times, discharge stability, discharge uniformity, and current density. These characteristics depend strongly on electron transport parameters, such as electron drift velocity, electron attachment, detachment and ionization coefficients as well as charge recombination rates. The electron transport parameters of various gases are thus needed for designing various discharge switches, and they are measured in this research program.

In addition to practical applications, this research program also develops new methods for the study of basic phenomena in

plasma physics. A high-charge-density plasma can be produced by an intense excimer laser pulse by the multiphoton-ionization process, and it can be used for examining the probability of electron leakage from plasma and the decay time of plasma in high gas pressures.

II. RESEARCH ACCOMPLISHMENTS

A parallel-plate drift-tube apparatus was used to investigate electron transport parameters in high pressure buffer gases. Electrons were initially produced either by irradiation of the cathode or by two-photon-ionization of a trace of trimethylamine in a high-pressure buffer gas with an intense excimer laser pulse. An electric field produced by applying a negative high voltage on the cathode was used to drift the electrons. The transient voltage pulses induced by electron motion between the electrodes were observed. The electron attachment rates were obtained from the ratio of the amplitudes of transient pulses with and without a gas attacher in buffer gas. The electron drift velocity and the electron diffusion coefficient were obtained by analyzing the time profile of transient pulses.

In this period, the two-photon-ionization coefficients of CS₂ and SO₂ at 193 nm were also measured. These coefficients are needed for determining the initial electron densities produced by laser-ionization of trace amounts of CS₂ and SO₂ in buffer gases. Results accomplished in this period are described more specifically below.

1. Electron Production from Photoionization of CS₂, SO₂ and (CH₃)₃N

The electron productions from photoionization of CS₂, SO₂, and (CH₃)₃N in buffer gases of N₂ and CH₄ with an ArF excimer laser (193 nm) were investigated. At low laser power and low gas pressure, the number of electrons produced are proportional to the square of laser power and the density of CS₂, SO₂ or (CH₃)₃N, indicating that electrons are produced by two-photon-ionization (TPI) process. The TPI coefficients for CS₂, SO₂ and (CH₃)₃N were measured to be 3.7×10^{-27} , 8.3×10^{-30} , and 1.7×10^{-27} cm⁴/W, respectively. The results are described in more detail in a paper attached in this report as Appendix A. This paper has been accepted by the Journal of Applied Physics for publication.

2. Space Charge Effect on Electron Transport

The probability for electron leakage from a plasma depends on the charge density and the applied field. The electron leakage probability decreases with charge density and increases with applied field. In an earlier observation of (CH₃)₃N, we find that the probability is a function of the ratio of charge density to the applied field. This phenomenon is repeatedly observed in the case of CS₂ which is briefly discussed in the paper attached as Appendix A.

The electron conduction pulse is greatly affected by the space charge effect. At high charge density, the electric field induced by the space charge can over-suppress the applied external field such that the conduction electrons move toward the cathode, and the electron conduction current reverses its

direction as shown in Fig. 9 in Appendix A. This new phenomenon is not expected from common belief that electrons should not move toward the cathode. However, this phenomenon has been observed in both cases of CS₂ and (CH₃)₃N whenever the electron density is high enough. We thus believe that this is a genuine physical phenomenon, although the theoretical explanation for this phenomenon is still not established. To understand this phenomena, theoretical modeling of the charge density and the time-dependent electric field is needed. We will continue to pursue this problem in the next funding period.

3. Electron Attachment Coefficients of H₂O

The electron attachment rate constants of H₂O in buffer gases of Ar, N₂ and CH₄ were measured as a function of E/N. The electron attachment rate constant of H₂O in Ar increases with E/N from 2 to 15 Td. This characteristic is desirable for the design of opening switches. For the H₂O-N₂ and H₂O-CH₄ gas mixtures, the electron attachment to H₂O is due to the formation of "temporary" negative ions, whose lifetime is about 200 ns. The formation of "temporary" negative ion has a certain effect on the electron drift velocity. The electron drift velocities of H₂O in various buffer gases were measured in this experiment.

The results for the electron attachment of H₂O in buffer gases are reported in more detail in a paper attached as Appendix B, which has been published in the Journal of Applied Physics.

4. Electron Attachment Coefficients of C₃F₈

The electron attachment coefficients of C₃F₈ in buffer gases of Ar, N₂, and CH₄ were measured as a function of E/N. The

electron attachment rate constants of C_3F_8 in N_2 and CH_4 increase with E/N , which are desirable for the design of opening switches. The electron drift velocity in the $C_3F_8-CH_4$ mixtures increases with increasing E/N , and it reaches a peak and then decreases at high E/N . The peak drift velocity shifts to high E/N as the C_3F_8 concentration increased. This characteristic satisfies the need for the design of opening switches.

The results for the shortening of electron conduction pulses by C_3F_8 are described in more detail in a paper attached as Appendix C, which has been published in the Journal of Applied Physics.

Accession For	
NTIS CRA&I	<input checked="" type="checkbox"/>
DTIC TAB	<input type="checkbox"/>
Unannounced	<input type="checkbox"/>
Justification	
By _____	
Distribution /	
Availability Codes	
Dist	Avail and/or Special
A-1	



III. CUMULATIVE PUBLICATIONS AND PRESENTATIONS

1. "Two-Photon-Ionization Coefficients of Propane, 1-Butene, Methylamines", L. C. Lee and W. K. Bischel, presented at the 12th International Conference on the Physics of Electronic and Atomic Collisions, Gatlinburg, TN, July 15-21, 1981.
2. "Electron Attachment and Charge Recombination Following Two-Photon-Ionization of Methylamines", L. C. Lee and W. K. Bischel, presented at the 34th Gaseous Electronics Conference, Boston, MA, October 20-23, 1981.
3. "Two-Photon-Ionization Coefficients of Propane, 1-Butene, and Methylamines", L. C. Lee and W. K. Bischel, J. Appl. Phys. 53, 203 (1982).
4. "Electron Ionization and Attachment Processes in Diffuse Discharges", L. C. Lee, presented to the Workshop on Optical Control of Diffuse Discharges, Eugene, OR, December 2-3, 1982.
5. "Diffusion of Electrons in Gases Under Electric Field", F. Li and L. C. Lee, presented at the 1983 Annual Meeting, APS Division of Electronic and Atomic Physics, Boulder, CO, May 23-25, 1983.
6. "Electron Longitudinal Diffusion Coefficients in Ar", F. Li and L. C. Lee, presented at the 36th Gaseous Electronics Conference, Albany, NY, October 10-14, 1983.
7. "Space Charge Effect on the Electron Kinetics Occurring in Atmospheric Gas Pressure", L. C. Lee and F. Li, presented at the 1984 IEEE International Conference on Plasma Science, St. Louis, Missouri, May 14-16, 1984.
8. "Shortening of Electron Conduction Pulses by Electron Attachments O_2 , N_2O and CF_4 ", L. C. Lee and F. Li, J. Appl. Phys., 56, 3169 (1984).
9. "Space Charge Effect on Electron Conduction Current", L. C. Lee and F. Li, paper submitted to IEEE Transactions on Plasma Science, 1984.
10. "Electron Attachment to C_3F_8 in High Pressure Buffer Gases" W. C. Wang and L. C. Lee, presented at the DEAP Meeting, American Physical Society, Norman, Oklahoma, May 29-31, 1985.
11. "Electron Attachment to H_2O in Ar, N_2 , and CH_4 in Electric Field", W. C. Wang and L. C. Lee, J. Appl. Phys. 57, 4360 (1985).

12. "Shortening of Electron Conduction Pulses by Electron Attacher C_3F_8 in Ar, N_2 , and CH_4 ", W. C. Wang and L. C. Lee, J. Appl. Phys. 58, 184 (1985).
13. "Shortening of Electron Conduction Pulses by Electron Attachers", L. C. Lee and W. C. Wang, presented at the IEEE Pulsed Power Conference, Arlington, VA, June 10-12, 1985.
14. "Electron Attachment to H_2O , SO_2 , and C_3F_8 in Ar, N_2 , and CH_4 " W. C. Wang, M. A. Fineman and L. C. Lee at XIV International Conference on the Physics of Electronic and Atomic Collisions, Palo Alto, CA, July 24-30, 1985.
15. "Electron Production by Photoionization of CS_2 and SO_2 at 193 nm" L. C. Lee and W. C. Wang, Accepted for presentation at the Thirty-Eighth Annual Gaseous Electronics Conference, Monterey, CA, Oct. 15-18, 1985.
16. "Electron Attachment to SO_2 and CS_2 in Ar, N_2 , and CH_4 ", W. C. Wang and L. C. Lee, Accepted for presentation at the Thirty-Eighth Annual Gaseous Electronics Conference, Monterey, CA, Oct. 15-18, 1985.
17. "Two-Photon-Ionization Coefficients of CS_2 , SO_2 and $(CH_3)_3N$ ", W. C. Wang and L. C. Lee, paper accepted for publication in J. Appl. Phys. (1985).

IV. PERSONNEL INVOLVED IN THIS RESEARCH

1. Principal Investigator:

Dr. Long C. Lee, Professor of Electrical & Computer Engineering

2. Dr. Morton A. Fineman, visiting Professor of Physics

3. Research Associates:

Dr. J. B. Nee
Dr. W. C. Wang

4. Students:

Mr. Chris Fagan
Mr. Mike Hom
Mr. Robert Tahimic
Mr. F. Mehran
Ms. M. Waxman

V. INTERACTIONS

1. We have constantly sent our papers to Dr. A. H. Guenther at the Air Force Weapons Laboratory, Dr. Alan Garscadden at the Air Force Wright Aeronautical Laboratory, Dr. M. Gundersen at the University of Southern California, Dr. J. T. Moseley at the University of Oregon, Dr. Bob Reinovsky at the Air Force Weapons Laboratory, Dr. S. K. Srivastava at the Jet Propulsion Laboratory, and Dr. K. Schoenbach at the Texas Tech University. We appreciate the useful comments and suggestions received from them.
2. The results obtained in the current funding period had been presented at (i) the DEAP Meeting, Norman, Oklahoma May 29-31, 1985; (ii) the IEEE Pulsed Power Conference, Arlington, VA, June 10-12, 1985; (iii) the XIV International Conference on the Physics of Electronic and Atom Collisions, Palo Alto, CA, July 24-30, 1985.
3. We had visited the Jet Propulsion Laboratory on Nov. 30, 1984 to discuss our results for the electron attachments to H₂O and C₃F₈ with Dr. S. K. Srivastava and Dr. A. Chutjian.

Appendix A

"Two-Photon-Ionization Coefficients of
CS₂, SO₂, and (CH₃)₃N"

Two-photon-ionization coefficients of CS₂, SO₂, and (CH₃)₃N

W. C. Wang and L. C. Lee

Department of Electrical and Computer Engineering, San Diego State University, San Diego, California 92182

(Received 8 May 1985; accepted for publication 15 July 1985)

Electrons produced by two-photon ionization of CS₂, SO₂, and (CH₃)₃N in N₂ and CH₄ buffer gases at 193 nm were investigated using a parallel-plate drift-tube apparatus. At a low charge density, the transient voltage induced by electron motion between the electrodes is proportional to the gas pressure and the square of laser power. The two-photon-ionization coefficients measured from the number of electrons produced are 3.3×10^{-27} , 8.3×10^{-30} , and 1.7×10^{-27} cm⁴/W for CS₂, SO₂, and (CH₃)₃N, respectively. The coefficient for (CH₃)₃N agrees with the earlier value measured using ion current. At a high charge density, the number of electrons observed deviates from the square dependence of laser power. The numbers of ions and electrons are greatly reduced by charge recombination whose reaction rate is enhanced in the presence of space charge.

← INDENT

← INDENT

I. INTRODUCTION

When molecules are irradiated by intense ultraviolet (UV) laser photons, high concentrations of charges can be produced. This charge production method has been used in several applications, for example: (i) in the development of laser-triggered discharge switches that have low jitters (1 ns)¹, (ii) in the measurements of electron attachment rate constants of various electronegative gases in high-pressure buffer gases,² and (iii) in the study of fundamental phenomena of electron leakage from a plasma.³ In these applications, the two-photon-ionization (TPI) coefficient is needed, because it determines the absolute charge density. In this paper, we report the TPI coefficients for molecules that have potential applications in electrical discharges.

Although the multiphoton ionization (MPI) process has been extensively applied in the study of atomic⁴ and molecular⁵ spectroscopy, there are relatively few measurements in absolute MPI coefficients. In most earlier MPI measurements⁶⁻⁹ positive ions were detected. In contrast, we measured the TPI coefficients here by detecting electrons. For a comparison with earlier measurements,⁸ the TPI coefficient of trimethylamine [(CH₃)₃N] was remeasured with this new method. This method is extended to measure the TPI coefficients of CS₂ and SO₂.

In the previous measurement⁸ of trimethylamine, the ion current was limited by charge recombination when the charge density was high. This charge recombination process was repeatedly studied in this experiment in a much shorter time scale, because electrons drift much faster than ions. We find that the charge recombination rate is greatly affected by space charge.³ The space charge can induce an internal electric field to cancel out the applied field. The effective electric field in the plasma region is thus reduced such that the electron energy decreases. Since the charge recombination rate is inversely proportional to the square root of electron energy,¹⁰ the reduction of electron energy by space charge will increase the charge recombination rate greatly. This enhanced charge recombination process is discussed in this paper.

II. EXPERIMENTAL

The experimental setup has been described in a previous paper.² In brief, excimer laser (Lumonics Model 861S) at 193 nm was used to photoionize molecules in a gas cell of 6-in. six-way aluminum cross. Only the central portion of the laser cross-sectional area perpendicular to the laser beam was used for the experiment, whose size was 6.2 mm perpendicular to the applied field and 13.1 mm along the field. A rectangular stop was used to define the beam area for which a fraction of about 65% of the laser beam was used in the experiment. The laser energy per pulse was measured right after the exit window (suprasil) of the cell by an energy meter (Scientech Model 365). For the study of laser power dependence, the laser power was uniformly reduced by inserting quartz plates in the laser path. The quartz plates were UV grade and polished so that they would presumably reduce the laser beam uniformly, namely, the beam profile was not affected by the plates. Two parallel plate electrodes made of stainless steel of 5 cm diameter and 4.5 cm apart were used to monitor the number of electrons. A negative high voltage was applied to the cathode. The electron current induced by the electron motion between the electrodes was converted into a transient voltage pulse across a resistor ($R = 100\text{--}1000 \Omega$) connecting the anode to ground. The transient voltage was monitored by a storage oscilloscope (HP Model 1727A) and photographed for permanent record.

The gas pressure (250–300 Torr) in the gas cell was maintained constant in a slow flow system (flow rate about 20 cm³STP/min). The flow system reduces the buildup of impurities released from walls or electrodes as well as those possibly produced from the photofragments of gases. The laser repetition rate was usually low (typically 0.5 Hz), such that the gas replacement rate was fast enough and the photofragments did not cause a serious problem. The gas pressure was measured by an MKS Baratron manometer. All measurements were done at room temperature.

Sulfur dioxide (SO₂) or carbon disulfide (CS₂) was diluted in N₂ or CH₄ before introducing into the gas cell filled with the buffer gas of N₂ or CH₄. The N₂ and CH₄ gases

(supplied by MG Scientific) have minimum purities of 99.998% and 99.99%, respectively. The SO_2 supplied by Matheson has a minimum purity of 99.98%. The CS_2 liquid (99.9% purity) was supplied by MCB Manufacturing Chemists, Inc. The CS_2 liquid contained in a stainless steel cylinder was pumped several hours at dry ice temperature to remove dissolved impurities before its vapor was used for experiment. The impurity level was believed to be very low, because the experimental results were reproducible in spite of the measurements carried out before or after an additional pumping. The impurities that possibly accompanied CS_2 vapor should not be more than 0.1%. A diluted trimethylamine (0.05% in prepurified N_2 supplied by Matheson) was used for the trimethylamine experiment.

III. RESULTS AND DISCUSSION

A. CS_2

Electrons produced by laser ionization of CS_2 were monitored by the transient current induced by electron motion between the electrodes. The transient current was measured by the voltage pulse across a resistor connecting the anode to ground. The transient voltage pulses for CS_2 - N_2 mixture at $E/N = 9.6 \text{ Td}$ ($1 \text{ Td} = 10^{-17} \text{ V cm}^2$) are shown in Fig. 1, where the laser energies were (a) 1.25, (b) 1.63, and (c) 2.19 mJ/pulse in the region between the electrodes, and the pressures of CS_2 and N_2 were 12 mTorr and 280 Torr, respectively.

As shown in Fig. 1(a), the measured voltage $V(t)$ is almost constant before $t = 1.5 \mu\text{s}$, and after this time the current starts to drop because electrons hit the anode. This transient pulse was produced by a low laser power, so the electron concentration was low and the measured voltage was only slightly affected by space charge. [Figures 1(b) and 1(c) show the effect of space charge and will be discussed later.] For the case of low charge density, the number of electrons produced by each laser pulse through the TPI process can be described as⁸

$$N_e(0) = \alpha \int_0^T I^2(t) dt n A l / h\nu, \quad (1)$$

where α (cm^4/W) is the TPI coefficient, I (W/cm^2) is the laser flux, n (cm^{-3}) is the concentration of the photoionized gas, A (0.81 cm^2) is the laser beam size, l (5 cm) is the laser path length between the electrodes, $h\nu$ is the photon energy (J), and T is the laser pulse duration.

The TPI coefficient can be determined from the electron number measured, if other quantities in Eq. (1) are known. The time profile of the laser pulse (supplied by the laser manufacturer) is used to determine $\int I^2 dt$, which is approximated by

$$\int_0^T I^2(t) dt = \sum_i I_i^2 \Delta t, \quad (2)$$

where I_i is the laser flux at every $\Delta t = 1 \text{ ns}$. The laser pulse width was about 10 ns, and the pulse profile was quite reproducible as specified by the manufacture. From shot to shot, the laser energy varied within 6%. Since only the central portion of the laser beam was used, the laser flux was assumed to be spatially uniform. This makes the A value in Eq. (1) equal to the laser beam size in the central region between the electrodes.

The number of electrons can be determined from the transient voltage as,

$$V(t) = i(t) R f(t), \quad (3)$$

where $i(t)$ is the transient current induced by electron motion, R is the resistor connecting the anode to ground, and $f(t)$ is the response of electronics which approaches unity when t is larger than the RC constant ($C \sim 3 \times 10^{-10} \text{ F}$). The R values used in the experiment were in the range of 100–1000 Ω , corresponding to RC constants of (3×10^{-8} – 3×10^{-7}) s.

The induced current depends on the number of electrons $N_e(t)$ and the electron drift velocity W as¹¹

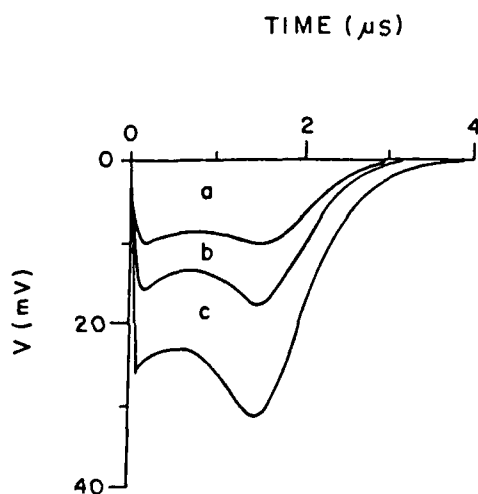


FIG. 1. The electron conduction pulses of CS_2 at $E/N = 9.6 \text{ Td}$, where electrons were produced by two-photon ionization of 12-mTorr CS_2 in 280-Torr N_2 buffer gas. The ArI laser energies were (a) 1.25, (b) 1.63, and (c) 2.19 mJ/pulse. The electrode spacing was 4.5 cm and the external resistor was 330 Ω .

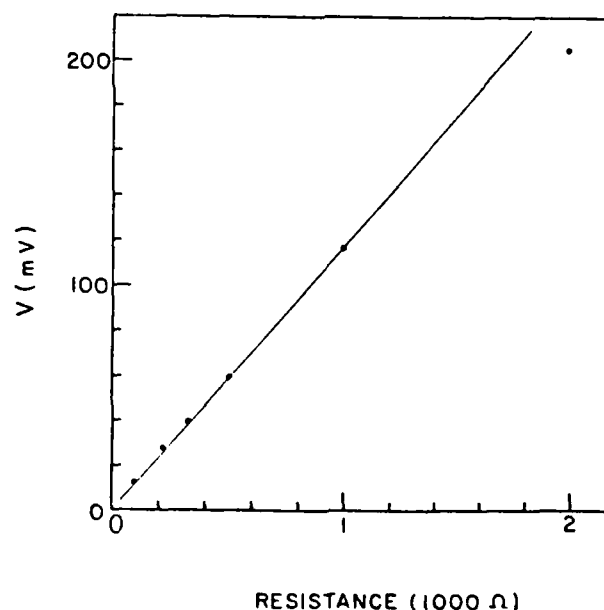


FIG. 2. The two-photon-ionization signal vs external resistor R . The data were taken with laser energy of 3.3 mJ/pulse, $E/N = 7.1 \text{ Td}$, $[\text{CS}_2] = 5 \text{ mTorr}$, and $[\text{N}_2] = 280 \text{ Torr}$.

$$i(t) = eN_e(t)W/d, \quad (4)$$

where d is the electrode spacing. In Eq. (4), we assume that all electrons are in equilibrium with the gas in the gas cell.

Substituting Eqs. (2)-(4) into (1), we have

$$V = \alpha(enARW) \sum_i I_i^2 \Delta t_i^2 / (nvd), \quad (5)$$

where V is measured at a time sufficiently long after the laser pulse such that $f(t) \rightarrow 1$ but before the electrons hit the anode such that $N_e(t) = N_e(0)$, namely, the V values were measured at the time shortly before electrons hit the anode.

In order to make certain that the measured V value was not affected by the response of electronics, we measured V as a function of R . The results are shown in Fig. 2, which were measured with a gas mixture of 5 mTorr CS₂ in 280 Torr N₂, $E/N = 7.1$ Td, and a laser energy of 3 mJ/pulse. As shown in Fig. 2, V is linearly dependent on R except at $R = 2 \times 10^3 \Omega$, where the measured V value is slightly lower than expected. This result indicates that the measured V values at $R < 10^3 \Omega$ are not affected by the response of electronics. The dependences of V on other parameters (such as electron drift velocity, laser flux, and gas pressure) are further checked below.

The electron drift velocities for various amounts of CS₂ or SO₂ in N₂ or CH₄ were measured as a function of E/N in this experiment, in which electrons were produced by irradiating the cathode with a KrF (248 nm) laser photons. (At this wavelength, the photon energy is not enough to ionize CS₂ and SO₂ by the TPI process.) The electrons produced by the cathode are well localized in space, so that the electron drift time is well defined. The electron drift velocity is equal to the electrode spacing divided by the electron drift time. Since the concentrations of CS₂ and SO₂ used in the measurements were so small that the electron drift velocities we measured for various gas mixtures were essentially the same as that of pure N₂ (Ref. 12) or CH₄ (Ref. 13) gas. More quantitatively,

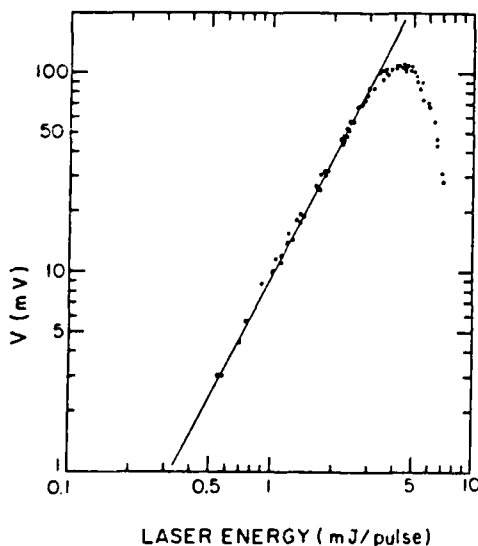


FIG. 3. The two-photon-ionization signal vs laser energy for CS₂ in N₂, where [CS₂] = 4.9 mTorr, [N₂] = 280 Torr, $E/N = 7.1$ Td, and $R = 1000 \Omega$.

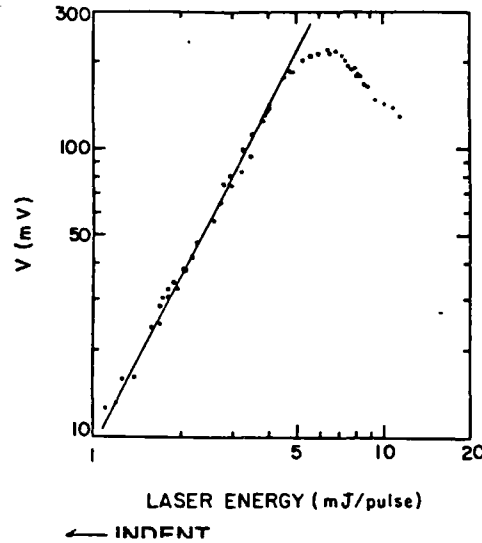


FIG. 4. The two-photon-ionization signal vs laser energy for CS₂ in CH₄, where [CS₂] = 7.3 mTorr, [CH₄] = 250 Torr, $E/N = 13.2$ Td, and $R = 100 \Omega$.

the electron drift velocity shows an observable change only when CS₂ in N₂ or CH₄ is more than 0.5%. In this experiment, the fraction of CS₂ was always smaller than 0.1%, thus, the electron drift velocity of the gas mixture was not different from the buffer gas.

The dependence of the observed voltage (which was measured at 1.5 μ s as shown in Fig. 1) on laser energy was investigated. The results for CS₂ (4.9 mTorr) in N₂ (280 Torr) are shown in Fig. 3, where $E/N = 7.1$ Td and $R = 1000 \Omega$. Each datum point in Fig. 3 represents a single laser pulse. At laser energies less than 3 mJ/pulse, V is linearly dependent on I^2 . This indicates that electrons are produced by the TPI process. At high laser energy, V deviates from the I^2 dependence. The V values decrease greatly at laser energies higher than 5 mJ/pulse. The decrease is caused by charge recombination and change of electron drift velocity which are enhanced by the space-charge effect (see discussion later). As noted before, the pulses shown in Figs. 1(b) and 1(c) have two maxima. We measure the V value at the later maximum, because it was less affected by the response of electronics and the space-charge effect.

Similarly, the dependence of voltage on laser energy was also investigated for the gas mixture of CS₂ (7.3 mTorr) in CH₄ (250 Torr) as shown in Fig. 4, where $E/N = 13.2$ Td and $R = 100 \Omega$. Again, at low laser energy, V is proportional to I^2 , and at high laser energy, V decreases with increasing laser energy. This decrease is again caused by charge recombination and change of electron drift velocity.

It should be noted that there was a background signal before CS₂ was added to the buffer gas in the gas cell. The background could be from the ionization of residual gas in the cell and/or from irradiation of the electrodes by stray laser light. The background signals were about the same for both N₂ and CH₄ buffer gases. The background signal was about 5% of the TPI signal of CS₂, and was subtracted out from the total signal. Thus the data shown in Figs. 3 and 4 are free from the background signal. It should also be noted that the laser energies shown in Figs. 3 and 4 are the true

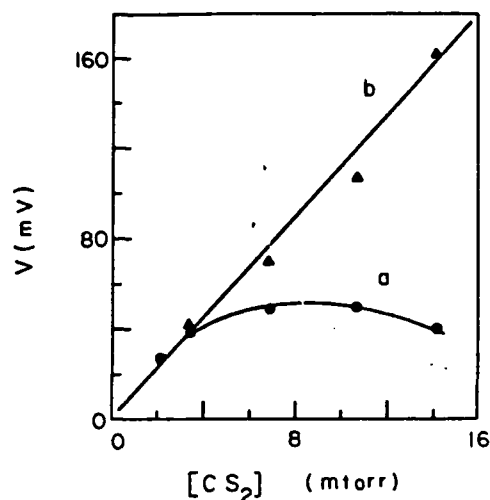


FIG. 5. The two-photon-ionization signal vs CS_2 gas pressure, where $[\text{CH}_4] = 250$ Torr, $E/N = 13.2$ Td, and $R = 100 \Omega$. (a), the laser energy in the central region between the electrodes is attenuated by CS_2 ; (b) the signals in (a) are corrected such that the laser energies are all equal to 3.1 mJ/pulse in the central region between the electrodes.

laser energies at the central region between the electrodes. The window transmission (about 90%) and the absorption of CS_2 have been corrected. The photoabsorption cross section of CS_2 at 193 nm measured here is $1.0 \times 10^{-16} \text{ cm}^2$, which is smaller than the value given by Rabalais *et al.*¹⁴ by a factor of about 2, but our value is consistent with the measurement of Suto and Lee¹⁵ using synchrotron radiation as a light source.

The dependence of the TPI signal on CS_2 pressure (in N_2 or CH_4 buffer gas) was investigated. As an example, the result of CS_2 in 250 Torr of CH_4 is shown in Fig. 5(a), where $E/N = 13.2$ Td, $R = 100 \Omega$, and the laser energy was kept constant at 3.1 mJ/pulse. Due to the attenuation of laser intensity by CS_2 , the laser energy in the central region of the gas cell decreases with increasing $[\text{CS}_2]$. Thus, the observed voltage is not linearly dependent on $[\text{CS}_2]$. However, if the photoabsorption of CS_2 is corrected such that the laser energies are the same, then the corrected V values become linearly dependent on $[\text{CS}_2]$ as shown in Fig. 5(b). Thus, our results are consistent with the expectation of Eq. (5) that V increases linearly with n .

From the above studies for the dependences of the observed voltages on the response of electronics, the laser flux, and the gas pressure, it is conclusive that the photoionization

is a two-photon process, and Eq. (5) is applicable for the case of low charge density. Thus, we can measure the TPI coefficient using the data taken at low laser energy and low CS_2 pressure. It should be noted that the loss of electrons by attachment to CS_2 at low pressure is negligible. This is justified by the fact that the transient pulse shown in Fig. 1(a) is flat in the 0–1.5- μs region. If the attachment process occurs, the transient voltage will decrease monotonically with time.² This assertion is consistent with the fact that the mean electron energies (< 1 eV)¹⁶ for N_2 and CH_4 at $E/N < 20$ Td are much lower than the dissociative electron attachment threshold for CS_2 (3.09 eV).¹⁷

The TPI coefficients measured with the CS_2 - N_2 and CS_2 - CH_4 gas mixtures are 3.4×10^{-27} and $3.1 \times 10^{-27} \text{ cm}^4/\text{W}$, respectively. These values are determined from the linear slopes shown in Figs. 3 and 4, corrected with the preabsorption of laser energy by CS_2 in Fig. 5. These coefficients along with the ionization potential¹⁸ and the single-photon absorption cross section of CS_2 at 193 nm measured in this experiment are listed in Table I. The TPI coefficients measured with various laser energies and gas pressures vary within the experimental uncertainty which is estimated to be $\pm 20\%$ of the average α value of $3.3 \times 10^{-27} \text{ cm}^4/\text{W}$. The sources of major experimental errors are (i) gas concentration (5%), (ii) electron drift velocity (10%), (iii) laser flux (5%), and (iv) background signal (1%).

The ionization potential of CS_2 is 10.08 eV.¹⁸ The energy of two ArF laser (6.42 eV/photon) photons is only sufficient to ionize CS_2 into CS_2^+ , but not energetically possible to produce other fragment ions such as CS^+ , S^+ , and S_2^+ . This is different from the observation of Seaver *et al.*¹⁹ that CS^+ was a major ion and significant amounts of S^+ , S_2^+ and CS_2^+ were produced from the multiphoton ionization of CS_2 at 193 nm and 266 nm. In their experiments, the lasers were focused and their laser flux of $10^{10} \text{ W}/\text{cm}^2$ was about four orders of magnitude higher than the flux used in this experiment. With such a high laser power, fragment ions can be produced by the stepwise photoabsorption processes. In each step the absorption can be saturated (i.e., all molecules are excited) such that the power dependence deviates from I^n , where n is the number of photons that are energetically possible to produce the observed fragment ion. For example, it requires three ArF laser photons to produce CS^+ , but the laser power dependence¹⁹ is only $n = 1.1$. Since our laser intensity is relatively low and the laser power dependence of

TABLE I. Two-photon-ionization coefficients α for CS_2 , SO_2 , and trimethylamine at 193 nm. Ionization potentials I. P. and single-photon absorption cross-sections σ at 193 nm are also listed.

Molecules	I. P. (eV)	σ (cm^2)	$\alpha(\text{cm}^4/\text{W})$		Ref. 8
			in N_2	in CH_4	
CS_2	10.08 ^a	1.0×10^{-16}	3.4×10^{-27}	3.1×10^{-27}	
SO_2	12.31 ^b	9.0×10^{-18}	8.6×10^{-30}	8.0×10^{-30}	
$(\text{CH}_3)_3\text{N}$	8.5 ^c	1.04×10^{-17d}	1.7×10^{-27}		1.5×10^{-27}

^a Reference 18.

^b Reference 22.

^c Reference 24.

^d Reference 8.

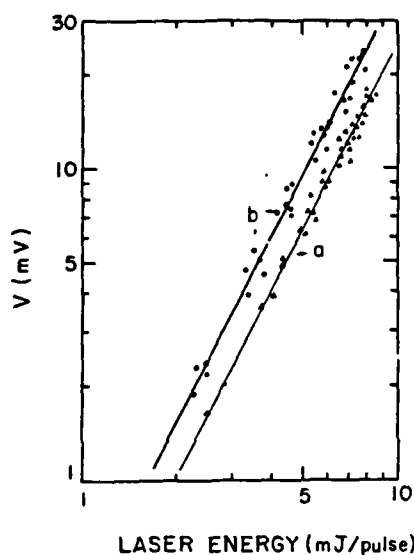


FIG. 6. The two-photon-ionization signal vs laser energy for SO_2 in N_2 and CH_4 . In (a), $[\text{SO}_2] = 33.6 \text{ mTorr}$, $[\text{N}_2] = 250 \text{ Torr}$, $E/N = 10.8 \text{ Td}$, and $R = 1000 \Omega$. In (b), $[\text{SO}_2] = 32 \text{ mTorr}$, $[\text{CH}_4] = 250 \text{ Torr}$, $E/N = 10.8 \text{ Td}$, and $R = 330 \Omega$.

electrons produced is I^2 , CS_2^+ is believed to be the major ion in our experiment.

We have tested the three-photon-ionization process using KrF laser photons at 248 nm (5.0 eV). The transient voltage signal was too small to be detectable. The upper limit of the three-photon-ionization coefficient of CS_2 at 248 nm was estimated to be $7 \times 10^{-39} \text{ cm}^6/\text{W}^2$.

B. SO_2

The transient voltages produced by two-photon ionization of SO_2 by various ArF laser energies are shown in Fig. 6. The data were taken with $[\text{SO}_2] = 33.6 \text{ mTorr}$, $[\text{N}_2] = 250 \text{ Torr}$, $E/N = 10.8 \text{ Td}$, and $R = 1000 \Omega$ for Fig. 6(a), and with $[\text{SO}_2] = 32 \text{ mTorr}$, $[\text{CH}_4] = 250 \text{ Torr}$, $E/N = 10.8 \text{ Td}$, and $R = 330 \Omega$ for Fig 6(b). In both cases, the transient vol-

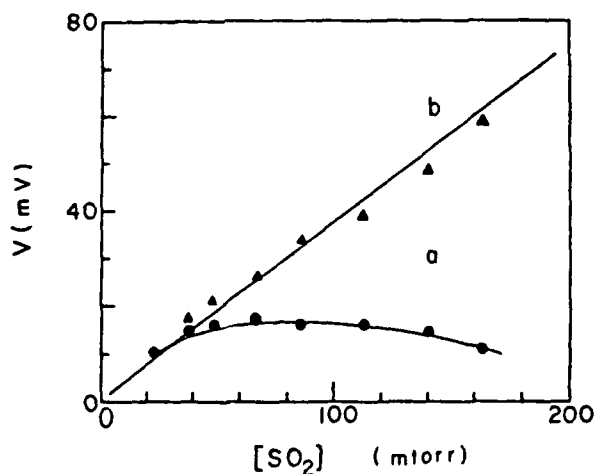


FIG. 7. The two-photon-ionization signal vs SO_2 gas pressure, where $[\text{N}_2] = 250 \text{ Torr}$, $E/N = 10.8 \text{ Td}$, and $R = 1000 \Omega$. The signals in (b) are corrected from (a) such that the laser energies at the central region between the electrodes are all equal to 7.21 mJ/pulse.

tages increase with the square of laser energy. This result again shows that electrons are produced by the TPI process. In contrast to CS_2 , there is no space-charge effect occurring at high-laser energy, because the TPI coefficient of SO_2 is so small that the charge density is always low.

The dependence of the TPI signal on the SO_2 pressure is shown in Fig. 7(a), where $[\text{N}_2] = 250 \text{ Torr}$, $E/N = 10.8 \text{ Td}$, laser energy = 7.21 mJ/pulse, and $R = 1000 \Omega$. Similar to the case of CS_2 , the TPI signals do not increase linearly with increasing $[\text{SO}_2]$, because the laser energy is preabsorbed by SO_2 . The absorption cross section measured at 193 nm is $9.0 \times 10^{-18} \text{ cm}^2$, which is comparable with the published value.²⁰ If the laser energy is corrected, the voltages produced by a same laser energy of 7.21 mJ/pulse are shown in Fig. 7(b). The voltages increase linearly with increasing $[\text{SO}_2]$ as expected from Eq. (5). The electron attachment to SO_2 is negligible, because the electron energy in N_2 or CH_4 ($< 1 \text{ eV}$)¹⁶ is too low to make the electron attachment occur. The threshold energy for the dissociative electron attachment process of SO_2 is about 3.5 eV.²¹

The TPI coefficients measured with the $\text{SO}_2\text{-N}_2$ and $\text{SO}_2\text{-CH}_4$ mixtures are 8.6×10^{-30} and $8.0 \times 10^{-30} \text{ cm}^4/\text{W}$, respectively. These values along with ionization potential^{22,23} and absorption cross section are listed in Table I. The values measured at various laser energies and gas pressures vary within experimental uncertainty which is estimated to be $\pm 20\%$ of the average α value of $8.3 \times 10^{-30} \text{ cm}^4/\text{W}$. This coefficient is more than two orders-of-magnitude smaller than that of CS_2 . The experimental error caused by the background signal is higher than that of CS_2 . However, the overall experimental uncertainties are not much different for both molecules, because the experimental error for the background signal is small when compared with other errors.

C. $(\text{CH}_3)_3\text{N}$

In order to compare with the earlier measurement, the TPI coefficient of trimethylamine was also measured in this experiment. For low laser energy, the voltages increase with the square of laser energy as expected. The dependence of the

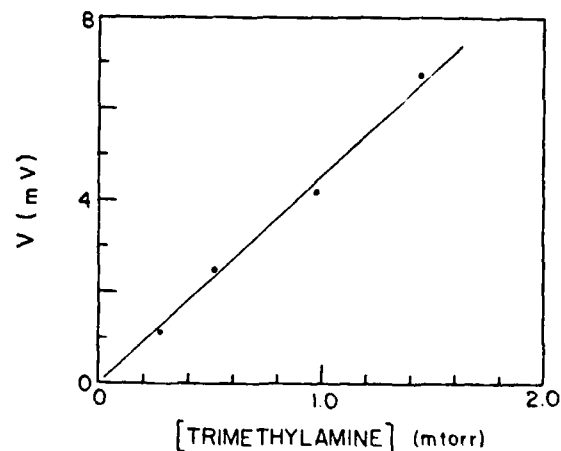


FIG. 8. The two-photon-ionization signal vs trimethylamine gas pressure, where $[\text{N}_2] = 280 \text{ Torr}$, $E/N = 7.06 \text{ Td}$, $R = 1000 \Omega$, and the laser energy of 2.06 mJ/pulse.

transient voltage on the trimethylamine pressure is shown in Fig. 8. The trimethylamine pressures are so low that the preabsorption of laser energy is negligible and the voltages increase linearly with gas pressure.

The measured α value is $1.7 \times 10^{-27} \text{ cm}^4/\text{W}$ as listed in Table I where the ionization potential²⁴ and the absorption cross section⁸ are also listed. The current α value agrees very well with the earlier measurement⁸ of $1.5 \times 10^{-27} \text{ cm}^4/\text{W}$, despite that these two measurements were carried out by different methods. In the earlier experiment⁸ the ion current was measured, and in this experiment we measured the number of electrons. The good agreement indicates that the present method is reasonably reliable.

It is of interest to note that at 193 nm, CS_2 has a TPI coefficient higher than trimethylamine by a factor of 2. Thus, similar to trimethylamine, CS_2 is also a good candidate for producing high-electron density in laser-controlled switches.

D. Charge recombination

It was observed⁸ that at high laser energy the ion current produced by two-photon ionization of trimethylamine was smaller than the value calculated from the I^2 dependence (see Fig. 3 in Ref. 8). The decrease of ion current was attributed⁸ to charge recombination. This process was further studied in a short time scale by monitoring the number of electrons between the electrodes.³ It was found that the electrons and ions in the plasma fronts initially drifted apart by the applied field could form a quasidipole to induce an internal electric field opposite the applied field. Depending on the charge density, the induced field could be large enough to suppress the applied field. Once the total electric field in the plasma region is reduced, the electron-ion recombination rate increases. This space-charge effect gives a reasonable explanation for the decreases of ions and electrons observed in the experiments of trimethylamine.^{3,8}

The space-charge-induced charge recombination process was again observed in the $\text{CS}_2\text{-N}_2$ gas mixture. Figure 1(a) shows a slight decrease in the central portion of the pulse. This minimum becomes more obvious in Figs. 1(b) and 1(c) when the laser energy increases from 1.25 mJ/pulse in Fig. 1(a) to 1.63 mJ/pulse in Fig. 1(b), and to 2.19 mJ/pulse in Fig. 1(c). When the laser energy further increases, the minimum can even change sign to positive.

Similar results were observed in the $\text{CS}_2\text{-CH}_4$ gas mixtures as shown in Fig. 9, where $[\text{CS}_2] = 7.2 \text{ mTorr}$, $[\text{CH}_4] = 257 \text{ Torr}$, and laser energies were 2.6, 5.5, and 8.0 mJ/pulse for Figs. 9(a), 9(b), and 9(c), respectively. The voltages of the first peak at a short time after the laser pulse increase with laser energy. But the second peak first increases with laser energy, and then decreases at high laser energy. (The laser energy dependences of the voltage for the second peak are shown in Figs. 3 and 4.) The minimum in the central portion of each pulse becomes deeper as the laser energy is sufficiently large. The voltage even changes sign when the laser energy is large enough as shown in Fig. 9(c). The voltage (or current) reverse means that the majority of electrons move toward the cathode instead of moving toward the anode by the applied field.

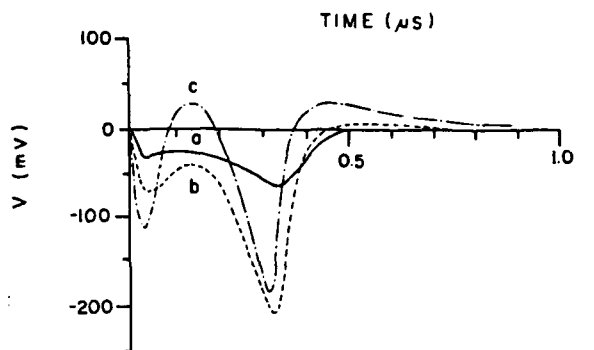


FIG. 9. The transient voltage pulses produced by the two-photon-ionization of CS_2 in CH_4 , where $[\text{CS}_2] = 7.3 \text{ mTorr}$, $E/N = 13.1 \text{ Td}$, $R = 100 \Omega$, and $[\text{CH}_4] = 257 \text{ Torr}$. The laser energies were (a) 2.6, (b) 5.5, and (c) 8.0 mJ/pulse.

The current reverse has been observed in an earlier trimethylamine experiment.³ This current reverse is likely caused by the space-charge effect, which will be described in detail in another paper. Here we present a brief scheme to explain the observed phenomena. The first peak in Fig. 9(c) was produced by the electrons initially produced by laser ionization and drifted in the applied field. As soon as electrons move, the electrons and the ions in the opposite plasma fronts form a quasidipole that produce an internal electric field in the direction opposite to the applied field. The total electric field in the plasma region, which is equal to the sum of the applied field and the space-charge-induced field, is thus reduced so that the electron drift velocity decreases. This explains the voltage decrease after the first peak.

The space-charge-induced electric field depends on the charge density. If the charge density is high enough, the induced field at some instant can be so large that it over suppresses the applied field. Namely, the total electric field can be in the direction opposite to the applied field such that the majority of electrons (which include the electrons both inside and outside the plasma region) move toward the cathode. This explains the change of voltage sign from negative to positive (current reverse) as shown in Fig. 9(c). As time proceeds, the charges in the plasma region may be lost by charge recombination and the space-charge-induced field may be weakened by a large separation of charges, thus the majority of electrons move toward the anode again. This explains the appearance of the second peak. After those electrons originally in the plasma front reach the anode, the current is dominated by the electrons in the plasma region that still move toward the cathode. This causes the change of voltage sign again from negative to positive (current reverse) after the second peak as shown in Figs. 9(b) and 9(c). (These results indicate that electrons carry a sufficient inertia momentum such that they do not respond instantaneously with the change of electric field.) The long decay time of the positive voltages as shown in Figs. 9(b) and 9(c) suggests that the loss of electrons is due to the charge recombination process. Although this scheme explains the observed current reverse qualitatively well, quantitative analysis to support this claim is necessary and will be studied further.

In the measurement of the TPI coefficients, the space-charge effect was kept as low as possible. This was accom-

plished by keeping the charge density low or increasing the applied electric field. The linear portions shown in Figs. 3, 4, and 6 obey the TPI process of square-laser-power dependence, so the observed voltages are presumably free from the space-charge effect. The TPI coefficients measured under such conditions should be independent of E/N applied, which were confirmed in our experiments.

IV. CONCLUDING REMARKS

The two-photon-ionization coefficients of CS_2 , SO_2 , and $(CH_3)_3N$ have been measured by observing the transient current induced by electron motion in high-pressure buffer gas (N_2 or CH_4). The dependence of the number of electrons on laser energy and gas concentration was investigated. At low charge density, the transient voltage is proportional to gas pressure and the square of laser energy. This shows that the charges are produced by a two-photon-ionization process whose coefficients are reported in this paper. At high charge density, the transient voltage is reduced by charge recombination whose reaction rate is enhanced in the presence of space charge.

ACKNOWLEDGMENTS

The authors wish to thank Dr. E. R. Manzanera, Dr. J. B. Nee, and Dr. M. Suto in our laboratory for useful suggestions and discussion. This work is supported by the Air Force Office of Scientific Research under Grant No. AFOSR-82-0314.

¹J. R. Woodworth, C. A. Frost, and T. A. Green, *J. Appl. Phys.* **53**, 4734 (1982).

²L. C. Lee and F. Li, *J. Appl. Phys.* **56**, 3169 (1984).

³L. C. Lee and F. Li, "Space Charge Effect on Electron Conduction Current" (unpublished).

⁴G. S. Hurst, M. G. Payne, S. D. Kramer, and J. P. Young, *Rev. Mod. Phys.* **51**, 767 (1979); C. H. Chen, G. S. Hurst, and M. G. Payne, *Chem. Phys. Lett.* **75**, 473 (1980).

⁵P. M. Johnson, *Appl. Opt.* **19**, 3920 (1980); P. M. Johnson and C. E. Otis, *Ann. Rev. Phys. Chem.* **32**, 139 (1981).

⁶J. H. Brophy and C. T. Rettner, *Chem. Phys. Lett.* **67**, 351 (1979).

⁷W. Zapka and F. P. Schafer, *Appl. Phys.* **20**, 287 (1979).

⁸L. C. Lee and W. K. Bischel, *J. Appl. Phys.* **53**, 203 (1982).

⁹G. A. Abakumov, B. I. Polyakov, A. P. Simonov, L. S. Tchuiko, and V. T. Yaroslavtzev, *Appl. Phys. B* **27**, 57 (1982).

¹⁰J. A. Rees, in *Electrical Breakdown of Gases*, edited by J. M. Meek and J. D. Craggs (Wiley, Chichester, UK, 1978), p. 70-76.

¹¹L. G. H. Huxley and R. W. Crompton, *The Diffusion and Drift of Electrons in Gases* (Wiley, New York, 1974).

¹²J. Dutton, *J. Phys. Chem. Ref. Data* **4**, 577 (1975).

¹³W. C. Wang and L. C. Lee, *J. Appl. Phys.* **57**, 4360 (1985).

¹⁴J. W. Rabalais, J. M. McDonald, V. Scherr, and S. P. McGlynn, *Chem. Rev.* **71**, 73 (1971).

¹⁵M. Suto and L. C. Lee (unpublished).

¹⁶L. G. Christophorou, *Atomic and Molecular Radiation Physics* (Wiley, New York, 1971).

¹⁷J. P. Ziesel, G. J. Schulz, and J. Milhaud, *J. Chem. Phys.* **62**, 1936 (1975).

¹⁸W. C. Price and D. M. Simpson, *Proc. R. Soc.* **165**, 272 (1938); Y. Tanaka, A. S. Jursa, and F. J. LeBlanc, *J. Chem. Phys.* **32**, 1205 (1960).

¹⁹M. Seaver, J. W. Hudgens, and J. J. DeMarco, *Chem. Phys.* **70**, 63 (1982); *Int. J. Mass Spectrom. Ion Phys.* **34**, 159 (1980).

²⁰D. Golomb, K. Watanabe, and F. F. Marmo, *J. Chem. Phys.* **36**, 958 (1962); D. E. Freeman, K. Yoshino, J. R. Esmond, and W. H. Parkinson, *Planet. Space Sci.* **32**, 1125 (1984).

²¹J. Rademacher, L. G. Christophorou, and R. P. Blaunstein, *J. Chem. Soc. Faraday Trans. II* **71**, 1212 (1975).

²²J. H. D. Eland and C. J. Danby, *Int. J. Mass Spectrom. Ion Phys.* **1**, 111 (1968); D. W. Turner, C. Baker, A. D. Baker, and C. R. Brundle, *Molecular Photoelectron Spectroscopy* (Wiley, London, 1970), pp. 84-86.

²³O. J. Orient and S. K. Srivastava, *J. Chem. Phys.* **80**, 140 (1984).

²⁴M. B. Robin, *Highly Excited States of Polyatomic Molecules, Vol. I and II* (Academic, New York, 1974).

FOOTNOTE
LINE LIMIT →

LIMIT OF TEXT

Appendix B

"Electron Attachment to H₂O in Ar, N₂ and
CH₄ in Electric Field"

Electron attachment to H₂O in Ar, N₂, and CH₄ in electric field

W. C. Wang and L. C. Lee

Department of Electrical and Computer Engineering, San Diego State University, San Diego, California 92182

(Received 25 October 1984; accepted for publication 19 December 1984)

The attachment of electrons to H₂O in Ar, N₂, or CH₄ is investigated using a parallel-plate drift-tube apparatus. Electrons are produced either by irradiation of the cathode with ArF laser photons or by two-photon-ionization of a trace of trimethylamine in a buffer gas. The transient voltage pulses induced by the electron motion between the electrodes are observed. The electron attachment rate of H₂O is determined from the ratio of transient voltage with and without H₂O added to the buffer gas. The measured electron attachment rate constants of H₂O in Ar increase with E/N from 2 to 15 Td. Electron attachment due to the formation of "temporary" negative ions in the H₂O-N₂ and H₂O-CH₄ mixture were observed. The lifetime of the negative ion was determined to be about 200 ns, whose nature is discussed. The "apparent" electron attachment rate constants for the formation of "temporary" negative ions in the H₂O-CH₄ gas mixture are measured for E/N from 1 to 20 Td. The electron drift velocities for the gas mixtures of H₂O in various buffer gases are measured.

I. INTRODUCTION

Recent advances in pulse-power technology indicate¹ that opening switches are needed for further developing a magnetic energy storage system. The inductive energy storage is preferable to the capacitive storage because the energy density in the inductive system is much higher (some 10²-10³ times) than the capacitive system.² Opening switch requires a fast decay of conduction current which could be achieved by attaching electrons to electronegative gases mixed in a buffer gas.¹ Thus, the electron attachment rates for various gas mixtures are needed for the development of this type of discharge switch. Our study of the electron attachment due to a small amount of H₂O in Ar, N₂, and CH₄ is reported in this paper.

The dissociative electron attachment process of water vapor has been studied extensively by the swarm method³⁻¹⁰ and the electron-beam method.¹¹ The predominant negative charged species are H⁻ and O⁻ ions with the onset energies of about 5.5 and 4.9 eV, respectively.^{12,13} Because these onset energies are high, the density-reduced electric field, E/N , in pure H₂O must be larger than 40 Td (1 Td = 10⁻¹⁷ V cm²) in order to have electron attachment occur. The E/N can be lower if Ar buffer gas is used, because for same E/N the electron energy¹² in Ar is higher than in H₂O. Earlier studies on the electron attachment have been summarized by Gallagher *et al.*¹⁴ Herein we report additional measurements on electron attachment rates for the dissociative attachment process of H₂O in Ar at varied electric fields.

Bradbury and Tatel¹⁵ observed an electron attachment in water vapor at low electron energy (less than 1 eV). The attachment probability increases with the H₂O concentration, [H₂O], and decreases with increasing E/N . A similar result was later reported by Kuffel.³ The attachment is attributed to nondissociative process that leads to the formation of negative ion. However, no long-lived H₂O⁻ ions were observed by several other works.^{7,10,12,16} This discrepancy could be reconciled if there exists a short-lived negative ion, as suggested by Hurst *et al.*^{17,18} From our observations we conclude that this short-lived negative ion does exist, as

evident by electrons being attached by H₂O in N₂ or CH₄ at low E/N .

In this work, we applied a relatively new method¹⁹ to investigate the electron attachment in mixtures of water vapor in Ar, N₂, and CH₄. The mean electron energies in the buffer gases decrease in the order of Ar, N₂, and CH₄ at each fixed E/N . For example, the mean electron energies at $E/N = 1.2$ Td are 2.53, 0.35, and 0.11 eV for Ar, N₂, and CH₄, respectively.¹² Thus, we were able to study the electron attachment process of water vapor over a wide range of electron energies (0.1-10 eV).

II. EXPERIMENT

In this experiment, electrons were produced by irradiation of the cathode with ArF laser photons which has a pulse duration of about 10 ns. The laser pulses are quite uniform in both the spatial and temporal distribution of photon fluxes. For the study of the H₂O-N₂ mixture, electrons were also produced by two-photon ionization (TPI) of a trace of trimethylamine present in the buffer gas using ArF laser photons. The experimental set-up has been discussed in detail in a previous paper.¹⁹ Briefly, the gas cell is a 6-in. six-way aluminum cross. The electrodes are two parallel stainless steel plates of 5 cm in diameter and 3.7 cm apart. The energy of ArF laser pulse (Lumonics Model 861S) was monitored by an energy meter (Sciencetech Model 365). A negative high voltage was applied to the cathode. The conduction current induced by the electron motion between the electrodes was observed as a transient voltage pulse across a resistor (220-1000 Ω) connecting the anode to ground. The transient pulse was monitored by a 275 MHz storage oscilloscope (HP Model 1727A). Each single transient pulse was stored in the oscilloscope which was later photographed for a permanent record. This experimental method is similar to that used by Verhaart and Van der Laan,²⁰ Christophoru *et al.*,²¹ and Aschwanden,²² for the electron ionization and electron attachment measurements.

The gas pressure in our gas cell was maintained constant in a slow flow system (flow rate ~ 20 cm³ STP/min). The

flow system reduces the buildup of impurities released from walls and electrodes as well as those produced from the photofragments of gases. The gas pressure (in the range of 200–500 Torr) was measured by an MKS Baratron manometer. All measurements were done at room temperature.

The Ar, N₂, and CH₄ gases (supplied by MG Scientific) have minimum purities of 99.998%, 99.998%, and 99.99%, respectively. To produce electrons by the TPI method, a diluted trimethylamine (0.05%) in prepurified nitrogen (supplied by Matheson) was used. All these gases were admitted to the gas cell without further purification. The water vapor was carried by Ar, N₂, or CH₄ into the gas cell. The concentration of H₂O was determined from the ratio of water vapor pressure (25 Torr at 26° C) to the pressure of carrier gases (> 1 atm). In order to remove the oxygen dissolved in the water, the water in a container was pumped periodically for several days before the water vapor was used for the experiment. The partial pressure of H₂O used in the experiment (< 5 Torr) was smaller than the water vapor pressure at room temperature. The carrier gas bubbled through the water, and the flow rate was kept low so that the equilibrium between the gas and the liquid of water exists in the water container. To ensure that the H₂O concentrations used to determine the rate constants are correct, we have also used a premixed gas mixture of H₂O (271 ppm) in Ar (supplied by Matheson) for the experiment. The attachment rate constants measured from both the premixed gas mixture and our water container are the same.

III. ANALYSIS METHOD

The method for the analysis of the data has been described in the previous paper.¹⁹ In brief, the current²³ induced by the electron motion is expressed as

$$i(t) = eN_e W / d, \quad (1)$$

where N_e is the number of electrons between the electrodes, W is the electron drift velocity, and d is the electrode spacing.

When water vapor is added to the gas cell, electron attachment by water molecules occurs, and current becomes

$$i'(t) = eN'_e W' e^{-v_a t} / d, \quad (2)$$

where v_a is the electron attachment rate of water vapor. Since the absorption coefficient of H₂O at 193 nm (ArF laser wavelength) is too small to attenuate the laser intensity, N'_e is essentially equal to N_e if the laser power is constant.

The current is converted to transient voltage by

$$V(t) = f(t)i(t)R, \quad (3)$$

where R is the resistor connecting the anode to the ground and $f(t)$ is the response function of the detection system that approaches constant as $t > RC$ (~ 60 ns). The logarithm of the ratio of the voltages with and without water vapor is thus

$$\ln(V'/V) = \ln(N'_e W' / N_e W) - v_a t. \quad (4)$$

For an atmospheric pressure and a relative low value of

E/N , electrons can reach an equilibrium state in a very short time. Thus, W and W' can be practically considered as constant except for those electrons near the electrodes. (At an Ar pressure of 400 Torr and an electric field of 100 V/cm, the relaxation time²³ for reaching an equilibrium is about 10 ns.) For $t < d/W$ (or d/W'), N_e (or N'_e) is a constant except for the beginning of the pulse where some electrons diffuse back to the cathode.²³ Therefore, after a reasonable time, the first term of Eq. (4) is independent of time, that is, the $V(t)$ is nearly constant. The plot of $\ln(V'/V)$ vs t thus gives the electron attachment rate v_a .

In the absence of water vapor, no attachment occurs. However, even if a small attachment due to impurities in the buffer gas does occur, the attachment can be included in the background and does not show in Eq. (4), namely, the measured v_a value is only due to the gas added (H₂O in this case).

When the electrons are produced from the laser irradiation of cathode, the electron drift velocity is equal to d/T , where T is the electron drift time between the electrodes which can be determined from the transient voltage waveform. In this experiment the mean electron drift time (0.4–4 μ s) is much longer than the duration of laser pulse (~ 10 ns), so the electrons are essentially all produced at $t = 0$. The effects of longitudinal and transverse electron diffusion on the measurements are neglected, since the gas pressures used in this experiment are quite high. For example, the ND_L value^{24–26} for Ar in the present E/N region is about $1.5 \times 10^{22} \text{ cm}^{-1} \text{ s}^{-1}$. For an Ar pressure of 200 Torr and an electron drift time of 1 μ s, the electron diffusion width ($\sqrt{2D_L t}$) is only about 0.07 cm. This is much smaller than the separation of electrodes ($d = 3.7$ cm). Therefore, the diffusion effect is not significant and is negligible in the data analysis. In any case, the diffusion effect does not affect the measurement of electron attachment rate constants, although it may slightly affect the electron drift velocity measurements.

If trimethylamine is used to produce electrons²⁷ as in the study of the H₂O–N₂ mixture, equal amounts of electrons and ions are produced by the TPI process in space. Since ions move much slower than electrons, ions can be considered as stationary in the time scale of interest, and Eq. (4) will thus be applicable in this case too. Nevertheless, the charge density should be kept low to avoid the space charge effect due to the charge-induced field.²⁸ For this case, the electron conduction current is very sensitive to the laser power fluctuation, because N_e is proportional to I^2 , where I is the laser intensity. The concentration of trimethylamine used in the experiment is usually small (< 1 mtorr), so its electron attachment rate is negligible (actually, the attachment due to trimethylamine is included in the background signal).

IV. RESULTS

A. H₂O–Ar mixture

The electron transient waveform $V(t)$ for the electron motion in 200 Torr of Ar at $E/N = 14.5$ Td is shown in Fig. 1(a). The pulse is a single shot, but it is a representative for

the means of several subsequent shots. From shot to shot, the pulse amplitudes vary within 10%. This variation is mainly caused by the fluctuation of laser energy. Nevertheless, the pulse shape is very reproducible, which meets the requirement for our measurements.

The voltage shown in Fig. 1(a) decreases rapidly after the first peak, which is due to the loss of electrons by back diffusion to the cathode.²³ The voltage approaches a nearly constant value as electrons move away from the cathode. The $V(t)$ starts to drop when electrons arrive at the anode. The time that $V(t)$ starts to drop is used to measure the drift time T . The amplitude shows a slight increase before it drops. This may be caused by the electrode effect, namely, electrons are accelerated more by the image charges when they move close to the anode. Since the gas pressure is high (200–400 Torr), the effect of electron diffusion is not large as stated before, and it may not affect the T value more than 10%. The electron drift velocity in both the pure Ar gas and the H₂O–Ar mixture as a function of E/N are plotted in Fig. 2. For pure Ar, our measured drift velocities are smaller than the published data,^{25,29,30} which are also plotted in Fig. 2 for comparison. The data of Hurst *et al.*⁵ for the Ar + H₂O mixtures are also plotted in Fig. 2, which are consistent with our measurements. Our data may be affected by the large electrical noise created by the laser discharge. The uncertainty for the $t = 0$ point is about 20 ns that may introduce an uncertainty of about 5% for the measured electron drift velocity.

When 0.073 Torr of H₂O is admitted to Ar at the same experimental condition of Fig. 1(a), the pulse duration and the amplitude decrease as shown in Fig. 1(b). The shortening of pulse duration indicates the increase of electron drift velocity and the decrease of amplitude is caused by the electron attachment to water vapor. (The electron drift velocities when adding H₂O to Ar at varied E/N are shown in Fig. 2.) The first peak in Fig. 1(b) is higher than that in Fig. 1(a), which again indicates the increase of electron drift velocity when H₂O is added to Ar. In fact, the amplitudes of the first peak at various water vapor concentrations are found to be linearly dependent on the electron drift velocity as expected from Eq. (4) for $t \sim 0$.

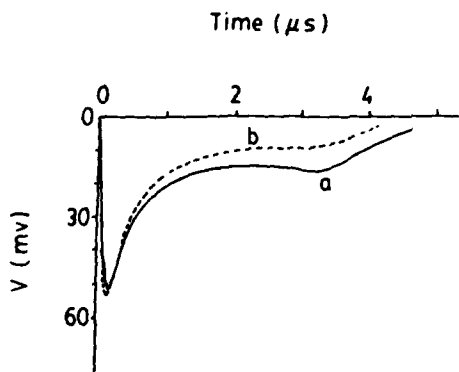


FIG. 1. The transient voltage waveforms produced from the electron motion in 200 Torr of Ar (a) without H₂O and (b) with 0.073 Torr of H₂O. The electrons were produced from irradiation of the cathode by ArF laser photons. The E/N was fixed at 14.5 Td, the electrode spacing was 3.7 cm, and the external resistor was 510 Ω .

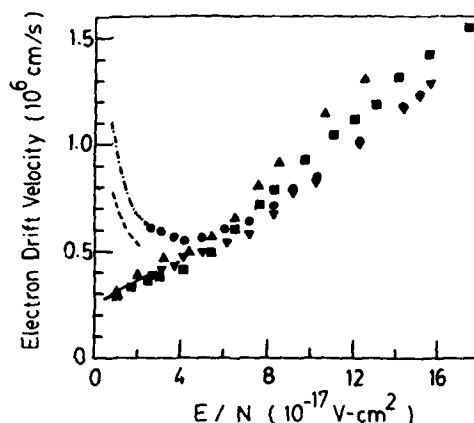


FIG. 2. The electron drift velocities as a function of E/N for the gases without (\blacktriangledown) and with 0.15% of H₂O (\bullet) in Ar. The electron drift velocity increases when H₂O is added to Ar. The data given by Errett (\blacksquare) and Nielson (\blacktriangle) for pure Ar and Hurst *et al.* for $[\text{H}_2\text{O}]/[\text{Ar}] = 0$ (—), 0.137% (---), and 0.25% (- - -) are plotted for comparison.

The flat portion ($1 < t < 3.3 \mu\text{s}$) in Fig. 1(a) indicates that the number of electrons drifting in space are constant and their drift velocities reach an equilibrium, namely, $N_e W = \text{const}$. The decrease of the voltage in the flat portion due to the addition of H₂O can thus be used for the measurement of electron attachment rate. During the period of the flat portion, the first term in Eq. (4) is independent of time and the plot of $\ln[V'(t)/V(t)]$ vs t gives v_a . The ratio of $V'(t)/V(t)$ at $E/N = 1.45$ Td for with and without 0.024, 0.048, and 0.073 Torr of H₂O in Ar are plotted in Figs. 3(a), 3(b), and 3(c), respectively. It is worth noting that the extrapolated value of V'/V at $t = 0$ increase with increasing H₂O concentrations. This is caused by the increase of electron drift velocity when H₂O is added to Ar as stated before. As shown in Fig. 3, $\ln(V'/V)$ is linearly dependent on t , and the electron attachment rate v_a is obtained from the slope.

The results for $v_a/[\text{H}_2\text{O}]$ as a function of $[\text{H}_2\text{O}]/[\text{Ar}]$ are shown in Fig. 4. At a fixed E/N , the $v_a/[\text{H}_2\text{O}]$ values decrease with increasing $[\text{H}_2\text{O}]/[\text{Ar}]$, which is likely caused⁵ by the effect of H₂O on the electron energy distribution in Ar. That is, an increase in $[\text{H}_2\text{O}]/[\text{Ar}]$ will decrease the number of electrons in the energy range where the dissociative attachment process will take place. The attachment

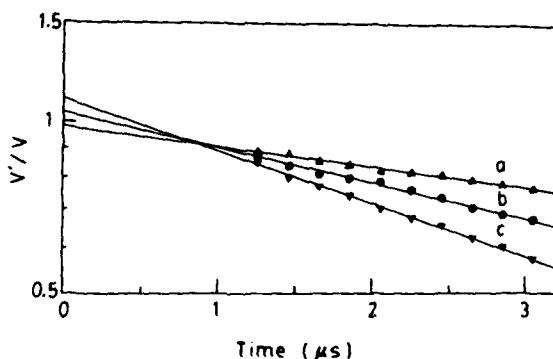


FIG. 3. The ratios of the transient voltages measured with and without H₂O in 200 Torr of Ar, V'/V , as a function of the elapsed time after laser pulse. The $[\text{H}_2\text{O}]$ are: (a) 0.024 Torr, (b) 0.048 Torr, and (c) 0.073 Torr. The E/N was fixed at 14.5 Td.

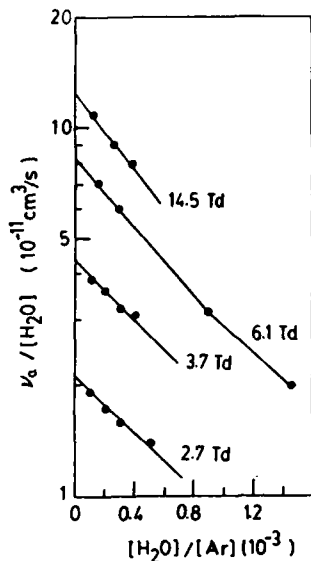


FIG. 4. The $v_a/[H_2O]$ values as a function of $[H_2O]/[Ar]$ for various applied E/N .

rate constants increase with increasing E/N at a constant $[H_2O]/[Ar]$.

The extrapolated value of $v_a/[H_2O]$ at $[H_2O] = 0$, $(v_a/[H_2O])_0$, is associated with the electron energy distribution in pure Ar. The electron attachment rate constants, $(v_a/[H_2O])_0$, as a function of E/N are shown in Fig. 5. No measurements were made below $E/N = 2.5$ Td, because at lower E/N the signal levels of $V(t)$ were too low to measure the attachment rates with certainty. The onset for the electron attachment rate constant is estimated (from the data shown in Fig. 5) to be at $E/N < 2$ Td. This result is consistent with the measurement of Hurst *et al.*⁵ that the onset is at $E/N = 1.2$ Td. However, the data of Hurst *et al.*⁵ (in the $E/N = 1-3$ Td region) do not join smoothly with the present data. A comparison is made in Sec. V.

At high E/N , the attachment rate constants do not increase as fast as those at low E/N as shown in Fig. 5. This may be accounted for by the fact that the mean electron energy in Ar does not increase at high E/N .¹² In addition, ionization may take place at high E/N which may interfere with the measurement of the electron attachment rate con-

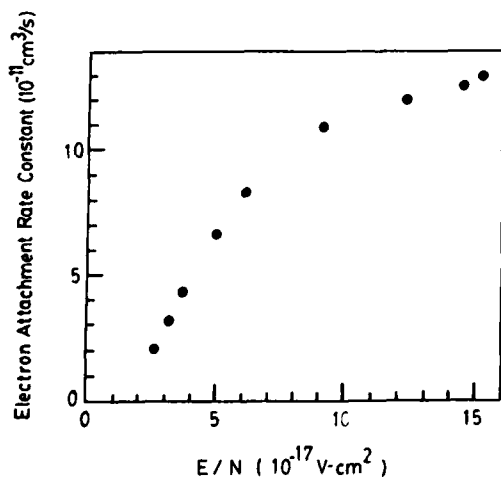


FIG. 5. Electron attachment rate constants obtained from the extrapolation of $v_a/[H_2O]$ at $[H_2O] = 0$ in the H_2O -Ar mixture as a function of E/N .

stant. For these reasons, we limited our measurements to E/N less than 15 Td.

In order to check the H_2O concentrations, as well as to avoid the problem of impurities which may be dissolved in water, the experiments were repeated using a premixed gas mixture of 271 ppm H_2O in Ar as the H_2O source. The results for the electron attachment rate constants are the same as above.

B. H_2O-N_2 mixture

For the H_2O-N_2 mixture, the transient waveforms observed with and without water vapor at E/N from 8 to 24 Td do not show difference. In this E/N region, the mean electron energy is in the range of 0.8-1.5 eV.^{12,25} These electron energies are too low for the dissociative attachment process,^{12,13} but too high for the nondissociative attachment process.^{3,15} Therefore, one does not expect the electron attachment process to occur.

When E/N is reduced, the waveforms with and without H_2O in N_2 show some differences. Two waveforms at $E/N = 6.3$ Td, one for 390 Torr of N_2 without H_2O and the other for 468 Torr of N_2 with 2.7 Torr of H_2O are shown in Figs. 6(a) and 6(b), respectively. These pulses are representatives for several subsequent shots. The waveforms are very reproducible, and the difference between Figs. 6(a) and 6(b) does have a statistical significance. As shown in Fig. 6(b), the pulse duration is shortened when H_2O is added, indicating that the electron drift velocity increases as H_2O is added. We have measured the electron drift velocities at various $[H_2O]$ and E/N , and found them to be consistent with the published data.¹⁸

Since the electron drift velocity increases with the addition of H_2O , it is expected that the first peak in Fig. 6(b) will be larger than that of Fig. 6(a). This expectation is different from the waveforms observed, namely, the amplitude of the first peak in Fig. 6(b) is smaller than that of Fig. 6(a). This result suggests that electron attachment occurs in this period. Furthermore, the amplitude of the second peak in Fig. 6(b) increases more than that of Fig. 6(a). This may result if the electrons attached earlier are released later to enhance the electron current at the end of the pulse. Comparing the amplitudes of Figs. 6(a) and 6(b), the current due to detachment appears at a time less than $0.7 \mu s$, indicating that the lifetime of this negative ion is less than this value.

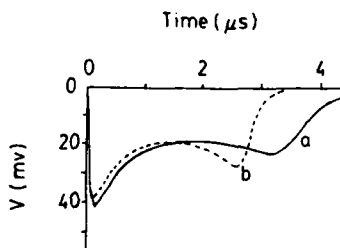


FIG. 6. The transient voltage waveforms produced from the electron motion in (a) 390 Torr of N_2 without H_2O and (b) 468 Torr of N_2 with 2.7 Torr of H_2O . The E/N was fixed at 6.3 Td. The electrode spacing was 3.7 cm, and the external resistor was 510Ω .

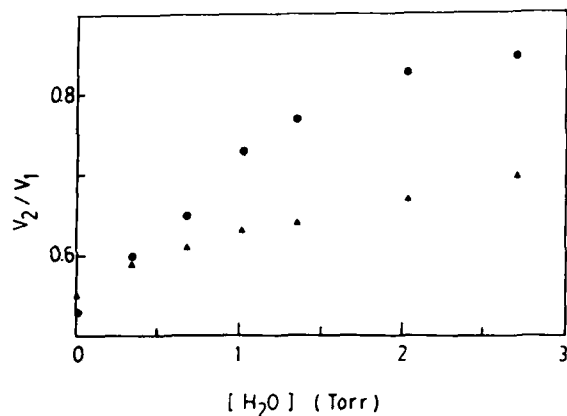


FIG. 7. The ratios for the magnitudes of the second peak to the first peak, V_2/V_1 , as a function of $[H_2O]$ in N_2 at $E/N = 4.2$ Td (●) and 6.3 Td (▲).

Because of the first peak and the second peak being affected by the attachment and detachment process of the temporary negative ion, the ratio of the amplitudes of these two peaks will give an indication for the attachment effect. For an example, the ratios for the amplitudes of the second peak V_2 to the first peak V_1 for the data taken at $E/N = 4.2$ and 6.3 Td at varied $[H_2O]$ are shown in Fig. 7. The V_2/V_1 values do not depend on E/N at $[H_2O] = 0$, but it shows dependence as $[H_2O]$ increased. The slope of the V_2/V_1 for $E/N = 4.2$ Td is larger than that for $E/N = 6.3$ Td. This suggests that the electron attachment rate for the formation of temporary negative ion increases with decreasing E/N . This is consistent with the earlier observations^{3,15} that the electron attachment rate for the nondissociative attachment process increases with decreasing electron energy. This phenomenon is further studied by measuring the electron attachment rate in the H_2O-CH_4 mixture below.

We have repeated the above experiments by producing the initial electrons by two-photon ionization of a trace of trimethylamine in N_2 . The results are consistent with the above experiments.

C. H_2O-CH_4 mixture

Two transient voltage waveforms at $E/N = 6.3$ Td, one for 324 Torr of CH_4 without H_2O and the other for 420 Torr of CH_4 with 3.6 Torr of H_2O are shown in Figs. 8(a) and 8(b), respectively. The pulse duration of $0.35 \mu s$ here is much shorter than that in Ar or N_2 gas. This is because the electron drift velocity in CH_4 is about one order of magnitude higher¹² than that in Ar or N_2 . The drift velocities as a function of E/N at various water vapor contents in CH_4 are shown in Fig. 9. It is noted that the electron drift velocity becomes smaller when H_2O is added to CH_4 , instead of larger as H_2O is added to Ar or N_2 . The electron drift velocities we measured agree well with the published data.¹⁸

In Fig. 8(b), the second peak is much smaller than the first peak [as compared with Fig. 8(a)], clearly indicating that an electron attachment due to H_2O occurs in this short pulse period. The electron attachment rate can be measured from the ratio of the voltages with and without H_2O in CH_4 . The ratios of V'/V for the H_2O pressures of 0.72, 2.16, and 3.59 Torr are plotted in Figs. 10(a) and 10(b) for $E/N = 2.5$

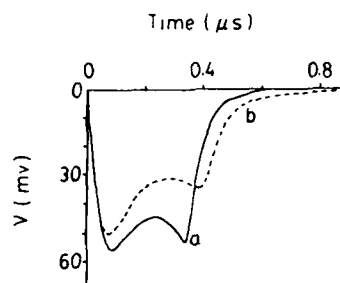


FIG. 8. The transient voltage waveforms produced from the electron motion in (a) 324 Torr of CH_4 without H_2O and (b) 420 Torr of CH_4 with 3.6 Torr of H_2O . The E/N was fixed at 5 Td, the electrode spacing was 3.7 cm, and the external resistor was 220Ω .

and 7.6 Td, respectively. For every case, $\ln(V'/V)$ is linearly dependent on t . The "apparent" electron attachment rates measured from the slopes at various $[H_2O]$ are shown in Fig. 11. At each E/N , the electron attachment rates increase linearly with $[H_2O]$, from which "apparent" electron attachment rate constants $\nu_a/[H_2O]$ are obtained as shown in Fig. 12. Note, the data were measured at several different CH_4 pressures. The attachment rate constants do not depend on the CH_4 pressure. It is also worth noting that the attachment is due to the formation of "temporary" negative ions, which is different from the "stable" ones. We thus call the measured attachment rate as an "apparent" one.

The second peak shown in Fig. 8(a) is significantly larger than the middle portion, indicating that in CH_4 the drift velocity for electrons near the anode is significantly affected by the electrode. For the measurements of attachment rates, the $[H_2O]$ concentrations were kept as low as possible so that the electron drift velocities were not significantly altered when H_2O was added. For the amount of H_2O (0.07–3.6 Torr) used in the experiment, the electron drift velocity at $E/N = 7.6$ Td is not significantly affected, which is reflected in Fig. 10(b) as the extrapolation of V'/V to $t = 0$ is nearly equal to 1. [The V'/V at $t = 0$ is proportional to W'/W as shown in Eq. (4).] At low E/N , the electron drift velocity depends strongly on the $[H_2O]$ added (see Fig. 9) so that the electron

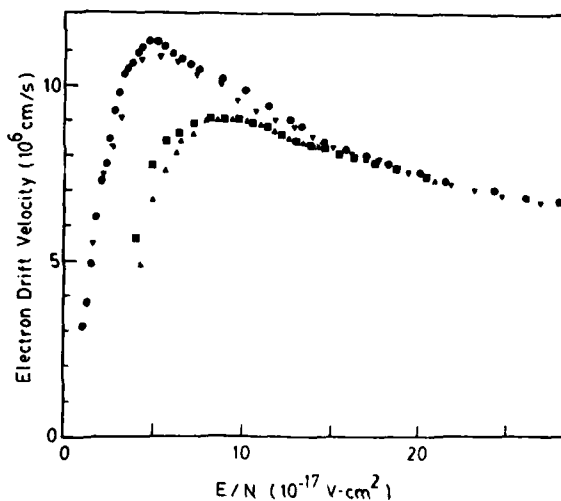


FIG. 9. The electron drift velocities in the H_2O-CH_4 mixtures as a function of E/N . The $[H_2O]/[CH_4]$ are: (●) 0%; (▼) 0.4%; (■) 1.2%; (▲) 1.7%.

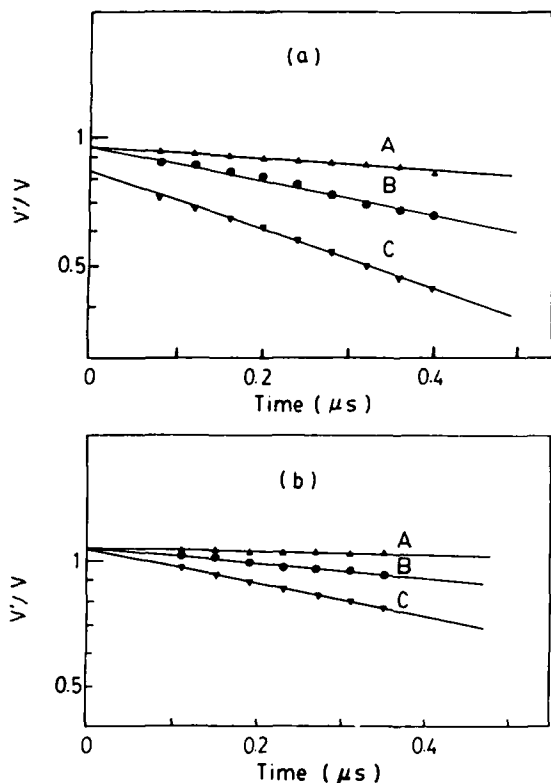


FIG. 10. The ratios of transient voltages measured with and without H_2O in CH_4 , V'/V , as a function of the elapsed time after the laser pulse at E/N of (a) 2.5 Td and (b) 7.6 Td. The gas pressures for H_2O in CH_4 are: (A) 0.72 Torr in 342 Torr; (B) 2.16 Torr in 379 Torr; (C) 3.59 Torr in 417 Torr.

drift velocity changes greatly with $[\text{H}_2\text{O}]$. However, the plot of $\ln(V'/V)$ is still linear as a function of t as shown in Fig. 10(a). The W'/W values determined from the extrapolation of V'/V at $t = 0$ with a correction of laser power fluctuation are consistent with the electron drift velocities measured from the pulse duration. This good agreement indicates that the present method is also applicable to electron attachment rate measurement even for the case where the electron drift velocity is changed by adding gases.

As shown in the measurements for the $\text{H}_2\text{O}-\text{N}_2$ mixture, the negative ion is a short-lived species, so that it will be detached later. Since the transient pulse in the $\text{H}_2\text{O}-\text{CH}_4$

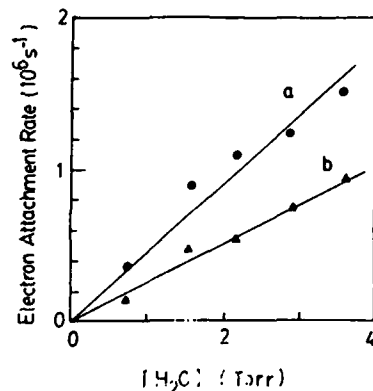


FIG. 11. "Apparent" electron attachment rate for $[\text{H}_2\text{O}]$ in $[\text{CH}_4]$ at E/N of (a) 2.5 Td (●) and (b) 7.6 Td (▲). The CH_4 pressures varied from 340 to 420 Torr as $[\text{H}_2\text{O}]$ increased.

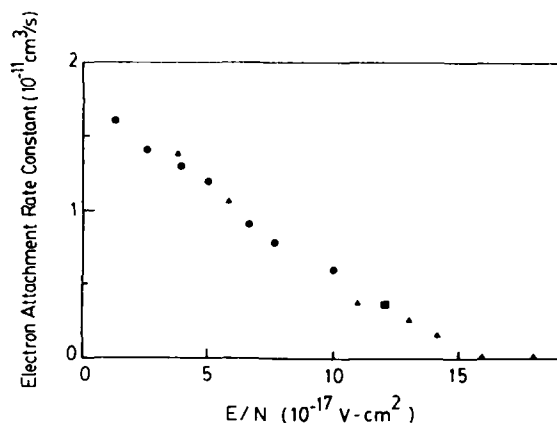


FIG. 12. "Apparent" attachment rate constants at various E/N for the $\text{H}_2\text{O}-\text{CH}_4$ mixture. The data were measured at the CH_4 pressures of 325 (●), 200 (▲), and 135 (■) Torr.

mixture is short, the current induced by the detached electrons may become observable after the primary electrons are absorbed by the anode. This expectation is indeed shown in the transient pulses of Fig. 8(b), in which the "after-current" of $V'(t)$ after $t = T'$ has a tail longer than that of $V(t)$ shown in Fig. 8(a) after $t = T$. The "after-currents" of $V(t)$ and $V'(t)$ are plotted on a logarithmic scale as shown in Figs. 13(a) and 13(b), respectively. The decay time in Fig. 13(a) is mainly the external RC time constant ($R = 220 \Omega$, $C \sim 3 \times 10^{-10} \text{ F}$). On the other hand, the after current shown in Fig. 13(b) has an additional long tail with a decay time of about 210 ns. This tail results from the detachment of the temporary ions, whose lifetimes vary in the range of 190–220 ns as measured at various $[\text{H}_2\text{O}]$ and E/N .

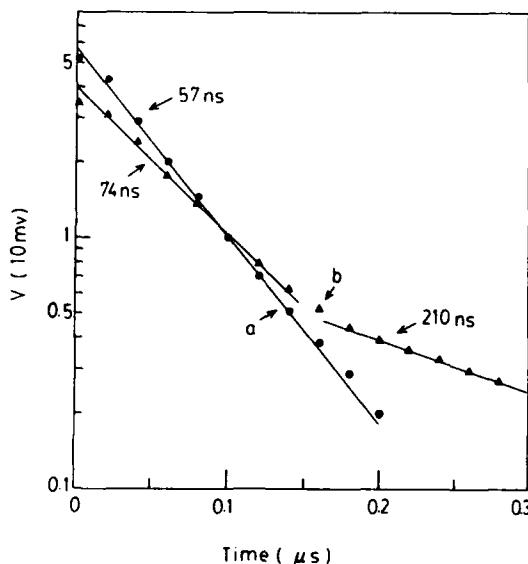


FIG. 13. The amplitudes of after-currents in Figs. 8(a) and 8(b) as a function of the time after primary electrons reaching the anode. The short decay times for both curves (a) and (b) are caused by the external RC circuit. The long decay time for (b) is caused by the electron detachment from the short-lived negative ion.

The electron detachment of the negative ions may affect the measurement of the electron attachment rate so that the measured attachment rate constant may appear low. However, the transient pulse duration in CH_4 (~ 400 ns) is not much longer than the lifetime of the temporary negative ion, also the concentration of negative ions is much less than that of primary electrons, so that the effect of detachment on the measured attachment rate may not be serious. It is estimated that the uncertainty of the attachment rate constant may not be larger than $\pm 30\%$ of the given value.

The earlier observations^{3,15} of electron attachment in H_2O at low electron energy were questioned^{12,14} because no stable H_2O^- ion was observed.^{7,10,12,16} The attachment was arbitrarily attributed^{12,14} to the presence of impurities, most likely O_2 . We have examined this impurity problem carefully. There are several observations to show that the attachment observed in this experiment is not due to O_2 . First, the negative ion observed is short-lived, in contrast to the O_2^- ion that is very stable. Second, the attachment is a two-body process as evident from the fact that the attachment rate constant is linearly dependent on $[\text{H}_2\text{O}]$ (see Fig. 12). This is quite different from the attachment process of O_2 which is a three-body process so that one would expect the attachment rate to be quadratically dependent on the gas pressure. Third, the attachment rates measured are quite high. It is unlikely that any impurity has such high concentration and high attachment cross section to make the attachment rate observable. These facts clearly indicate that the attachment is not caused by the possible impurity, O_2 , but is caused by the formation of temporary ions. This point is further discussed below.

V. DISCUSSION

The electron attachment rate constants are plotted versus the electron characteristic energies (D/μ) in CH_4 , H_2O , and Ar as shown in Fig. 14. The electron characteristic energy in CH_4 at each E/N is calculated from the data given by Cochran and Forester.³¹ The electron attachment rate constant for pure H_2O without buffer gas is obtained from the product of the electron attachment coefficient and the electron drift velocity at each E/N .¹⁴ The electron attachment coefficient for pure H_2O is the arithmetic mean value given by various investigators^{6,8,32,33} at each E/N as reviewed by Gallagher *et al.*¹⁴ The electron drift velocity and the electron characteristic energy for pure H_2O at each E/N are also adopted from this review paper.¹⁴ The electron characteristic energy for Ar at each E/N is obtained from a review paper given by Dutton.²⁵ The electron attachment rate constants measured by Hurst *et al.*⁵ in Ar at low E/N are also plotted for comparison.

As stated before, the electron attachment in H_2O at low electron energy reported before^{3,15} was subject to question.¹⁴ In order to resolve the discrepancy, Hurst *et al.*¹⁷ proposed earlier that H_2O might quasitrap low energy electrons, for which the "quasitrap" H_2O^- may have a limited lifetime in the order of 10^{-8} – 10^{-7} s. Later, in order to explain the measured momentum transfer cross section for H_2O being larger than the theoretical value by a factor of 2,

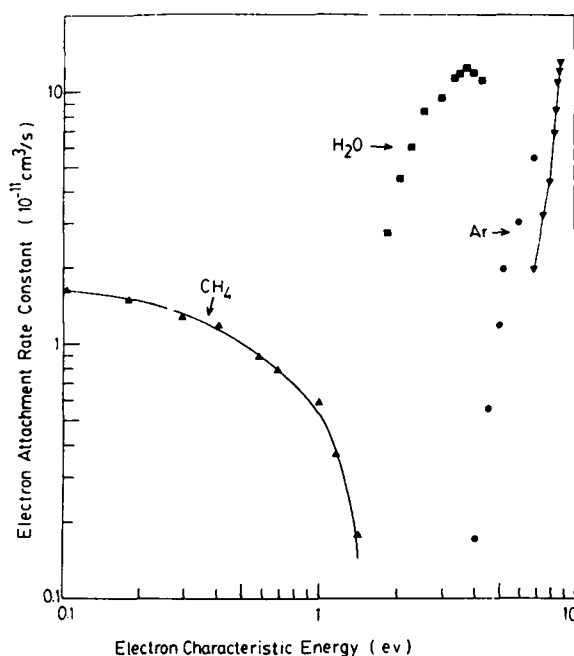


FIG. 14. Electron attachment rate constants as a function of electron characteristic energy in CH_4 , H_2O , and Ar. The data for H_2O in CH_4 (\blacktriangle) and Ar (\blacktriangledown) were measured in this experiment. The data for pure H_2O (\blacksquare) (from Ref. 14) and for H_2O -Ar (\bullet) (from Ref. 5) are plotted for comparison.

Hurst *et al.*¹⁸ repropounded that the motion of low energy electrons in H_2O may form a temporary negative ion. The formation of temporary negative ions has been used to explain¹⁸ the decrease of electron drift velocity as H_2O is added to CH_4 (see Fig. 9). The temporary ion of lifetime about 200 ns observed in this experiment fits very well with the suggestion.¹⁸

H_2O is a strong electron-polar molecule, the cross section for the rotational excitation by low energy electrons is very large (larger than 10^{-16} cm^2).^{34,35} The cross section for the vibrational excitation of H_2O by low energy electrons (< 1 eV) was also observed to be very large (peak $\sim 4 \times 10^{-16}$ cm^2).³⁶ The large excitation cross section was attributed to the dipole-dominated resonances.^{36,37} [The H_2O^- ($^2\text{A}_1$) state calculated by Claydon *et al.*³⁸ of about 2 eV is too high to be involved in the observed attachment.] It is presumed that H_2O is excited by low energy electrons to an intermediate compound state, $(\text{H}_2\text{O}^-)^*$, which then autodetaches to excited vibrational and rotational levels of the H_2O ground electronic state. The mechanism has been described in detail by Schulz for the diatomic molecules.³⁹ The lifetime of a compound state is usually short (10^{-10} – 10^{-15} s),³⁹ and it is not expected to be observable in our experiment. However, H_2O has a strong dipole moment, its compound state may live long enough such that it can collide with other H_2O molecules to form a dimer $\text{H}_2\text{O}^- \cdot \text{H}_2\text{O}$ or clusters $\text{H}_2\text{O}^- \cdot (\text{H}_2\text{O})_n$. The ion cluster is generally more stable⁴⁰ than the compound state. The temporary negative ions observed in this experiment may be dimers or clusters. Therefore, the lifetime observed may belong to the clusters instead of H_2O^- . The measured electron attachment rates for the formation of temporary negative ions depend linearly on $[\text{H}_2\text{O}]$ (see Fig. 11) and not on

[CH₃] (see Fig. 12). This indicates that the rate for the formation of clusters from the (H₂O⁻)* compound state may be very fast so that the primary electron attachment to H₂O is the rate controlling process.

For high energy electrons, the attachment is due to a dissociative attachment process. The attachment rate constants measured in Ar indicate that the attachment begins at a mean electron energy of about 4 eV. This is consistent with the thresholds^{12,13} for producing O⁻ and H⁻ from dissociative attachment of H₂O (i.e., 4.9 and 5.5 eV, respectively). The attachment rate constants reported by Hurst *et al.*⁵ are higher than the present values (see Fig. 14). The reason for this discrepancy is not known. The dissociative attachment process has been used to explain the observation that the addition of water vapor to dry air increases the breakdown voltage.³

The magnitude of the attachment rate constant for electrons in pure water is about the same as that in Ar as shown in Fig. 14, indicating that the electron attachment in H₂O is due to the dissociative attachment process. However, the mean electron energy in H₂O in Fig. 14 is less than the threshold for the O⁻ or H⁻ formation. This result suggests that the electron energy distribution in H₂O may be broad, and/or the mean electron energy is not well measured. Because the electron attachment rate constants are nearly the same for both H₂O-Ar and pure H₂O, it is likely that the electron energy in H₂O is not much broader than Ar, although the possibility of a wide energy spread in H₂O is not ruled out. The attachment at an electron energy lower than threshold may suggest that the published data for the mean "electron energy" in H₂O are too low. The mean electron energy in H₂O has not been studied too thoroughly to date.¹⁴

VI. CONCLUDING REMARKS

We have applied a different approach to investigate the transient electron conduction current in the gas mixture of a trace of H₂O in Ar, N₂, and CH₄. This method is different from the conventional swarm method in which negative ions are detected. We have demonstrated in this paper and a previous paper¹⁹ that the present method is useful for measuring the "apparent" electron attachment rate constants due to the formation of short-lived species.

For an opening switch, the electron attachment rate during the opening period needs to be high, that is, the electron attachment rate is required to increase with increasing E/N . The results of our experiment show that the H₂O-Ar mixture has this characteristic. The increase of the electron drift velocity due to the addition of H₂O to Ar is an additional benefit for the design of opening switch, because the electron conduction current will be increased during the switching period.

ACKNOWLEDGMENTS

The authors wish to thank Professor K. Schoenbach and Professor G. Schaefer at the Texas Tech University, Pro-

fessor M. A. Fineman at San Diego State University, and Dr. E. R. Manzanares, Dr. J. B. Nee, and Dr. M. Suto in our laboratory for useful suggestions and discussion. This work is supported by the Air Force Office of Scientific Research, Air Force Systems Command, USAF, under Grant No. AFOSR-82-0314.

- ¹K. Schoenbach, G. Schaefer, M. Kristiansen, L. L. Hatfield, and A. H. Guenther, *Electrical Breakdown and Discharges in Gases, Part B*, edited by E. E. Kunhardt and L. H. Luessen (Plenum, New York, 1983), p. 415.
- ²J. K. Burton, D. Conte, R. D. Ford, W. H. Lupton, V. E. Scherrer, and I. M. Vitkovitsky, *Digest of Technical Papers*, 2nd IEEE International Pulsed Power Conference, Lubbock, TX, edited by A. Guenther and M. Kristiansen, (IEEE, New York, 1979), p. 284.
- ³E. Kuffel, *Proc. Phys. Soc. London* **74**, 297 (1959).
- ⁴A. N. Prasad and J. D. Craggs, *Proc. Phys. Soc. London* **76**, 223 (1960).
- ⁵G. S. Hurst, L. B. O'Kelly, and T. E. Bortner, *Phys. Rev.* **123**, 1715 (1961).
- ⁶R. W. Crompton, J. A. Rees, and R. L. Jory, *Aust. J. Phys.* **18**, 541 (1965).
- ⁷J. L. Moruzzi and A. V. Phelps, *J. Chem. Phys.* **45**, 4617 (1966); J. L. Pack and A. V. Phelps, *J. Chem. Phys.* **45**, 4316 (1966).
- ⁸J. E. Parr, and J. L. Moruzzi, *J. Phys. D* **5**, 514 (1972).
- ⁹C. E. Klots and R. N. Compton, *J. Chem. Phys.* **69**, 1644 (1978).
- ¹⁰J. L. Pack, R. E. Voshall, and A. V. Phelps, *Phys. Rev.* **127**, 2084 (1962).
- ¹¹I. S. Buchel'nikova, *Zh. Eksp. Teor. Fiz.* **35**, 1119 (1958) [*Sov. Phys. JETP* **35**, 783 (1959)].
- ¹²L. G. Christophorou, *Atomic and Molecular Radiation Physics* (Wiley, New York, 1971).
- ¹³H. Massey, *Negative Ions* (Cambridge U. P., London, 1976), p. 347.
- ¹⁴J. W. Gallagher, E. C. Beaty, J. Dutton, and L. C. Pitchford, *J. Phys. Chem. Ref. Data* **12**, 109 (1983).
- ¹⁵N. E. Bradbury and H. E. Tatel, *J. Chem. Phys.* **2**, 835 (1934).
- ¹⁶J. F. Wilson, F. J. Davis, D. R. Nelson, R. N. Compton, and D. H. Crawford, *J. Chem. Phys.* **62**, 4204 (1975).
- ¹⁷G. S. Hurst, L. B. O'Kelly, and J. A. Stockdale, *Nature* **195**, 66 (1962).
- ¹⁸G. S. Hurst, J. S. Stockdale, and L. B. O'Kelly, *J. Chem. Phys.* **38**, 2572 (1963).
- ¹⁹L. C. Lee and F. Li, *J. Appl. Phys.* **56**, 3169 (1984).
- ²⁰H. F. A. Verhaar and P. C. T. Van der Laan, *J. Appl. Phys.* **53**, 1430 (1982); **55**, 3286 (1984).
- ²¹L. G. Christophorou, J. G. Carter, and D. V. Maxey, *J. Chem. Phys.* **76**, 2653 (1982).
- ²²Th. Aschwanden, *Gaseous Dielectrics IV*, *Proc. 4th Int. Symp. Gaseous Dielectrics*, edited by L. G. Christophorou (Pergamon, New York, 1984), pp. 24-33.
- ²³L. G. H. Huxley and R. W. Crompton, *The Diffusion and Drift of Electrons in Gases* (Wiley, New York, 1974), pp. 298-303.
- ²⁴F. Li and L. C. Lee, unpublished.
- ²⁵J. Dutton, *J. Phys. Chem. Ref. Data* **4**, 577 (1975).
- ²⁶E. B. Wagner, F. J. Davis, and G. S. Hurst, *J. Chem. Phys.* **47**, 3138 (1967).
- ²⁷L. C. Lee and W. K. Bischel, *J. Appl. Phys.* **53**, 203 (1982).
- ²⁸L. C. Lee and F. Li, unpublished.
- ²⁹D. D. Errett, "The Drift Velocity of Electrons in Gases," thesis, Purdue University, W. Lafayette, IN (1981).
- ³⁰R. A. Nielsen, *Phys. Rev.* **50**, 950 (1936).
- ³¹L. W. Cochran and D. W. Forester, *Phys. Rev.* **126**, 1785 (1962).
- ³²H. Ryzko, *Ark. Fys.* **32**, 1 (1966).
- ³³A. V. Ribbud and M. S. Naidu, *J. Phys. (Paris) Colloq.* **C7 40**, 77 (1979).
- ³⁴Y. Itikawa, *J. Phys. Soc. Jpn.* **32**, 217 (1972).
- ³⁵K. Jung, Th. Antoni, R. Muller, K. H. Kochem, and H. Ehrhardt, *J. Phys. B* **15**, 3535 (1982).
- ³⁶G. Seng and F. Linder, *J. Phys. B* **9**, 2539 (1976).
- ³⁷S. F. Wong and G. J. Schulz, *Proceedings of the 9th International Conference on Physics of Electronic and Atomic Collisions* (University of Washington, Seattle, 1975).
- ³⁸C. R. Claydon, G. A. Segal, and H. S. Taylor, *J. Chem. Phys.* **54**, 3799 (1971).
- ³⁹G. J. Schulz, *Rev. Mod. Phys.* **45**, 423 (1973).
- ⁴⁰S. G. Lias and P. Ausloos, *Ion-Molecule Reactions* (American Chemical Society, Washington, DC, 1975), pp. 165-197.

Appendix C

"Shortening of Electron Conduction Pulses
by Electron Attacher C_3F_8 in Ar, N_2 and CH_4 "

Shortening of electron conduction pulses by electron attacher C_3F_8 in Ar, N_2 , and CH_4

W. C. Wang and L. C. Lee

Department of Electrical and Computer Engineering, San Diego State University, San Diego, California 92182

(Received 19 February 1985; accepted for publication 19 March 1985)

The attachment rate constants of C_3F_8 in the buffer gases of Ar, N_2 , and CH_4 are measured using a parallel-plate drift-tube apparatus. The dependences of the electron drift velocities on the contents of C_3F_8 in various buffer gases are investigated. Electrons are produced by irradiating the cathode with ArF laser photons. The transient voltage pulses induced by the electron motion are observed. We find that the C_3F_8 - CH_4 mixture has the desirable characteristics of both electron drift velocity and attachment rate constant for the application of diffuse-discharge opening switches.

I. INTRODUCTION

It has been pointed out that fast opening switches are needed^{1,2} for developing a magnetic energy storage system.³ For the design of a fast opening switch, the duration of the electron conduction pulse and the electron drift velocity are the important parameters. The pulse duration can be shortened by attaching electrons to electronegative gases in various buffer gases. A gas mixture suitable for a diffuse-discharge opening switch has to fulfill the requirements^{1,2,4}: (i) high electron drift velocity and low electron attachment rate at low density-reduced electric field ($E/N \sim 3 \times 10^{-17}$ V cm²), and (ii) low electron drift velocity and high electron attachment rate at high E/N . In our research program, we have developed a method to measure the electron attachment rates and electron drift velocities of various gas mixtures for the application of opening switches.

Recently, Christophorou's group⁴⁻⁸ have measured the electron attachment rates and electron drift velocities for various binary gas mixtures by a swarm method. Among these gas mixtures, C_3F_8 -Ar and C_3F_8 - CH_4 were suggested as the good candidates for diffuse-discharge opening switches. In this paper we report the electron transport parameters of these mixtures using a different method. [We have already applied this method to measure the electron attachment rates of various gas mixtures such as N_2O - N_2 (Ref. 9) and H_2O -Ar (Ref. 10).] From our results in this study, we found that in the case of low C_3F_8 concentration the C_3F_8 - CH_4 and C_3F_8 - N_2 mixtures are suitable for the application of opening switches, but the C_3F_8 -Ar mixture is not.

II. EXPERIMENT

The experimental apparatus and the technique for data analysis have been described in detail in previous papers.^{9,10} Briefly, the gas cell is a 6 in. six-way aluminum cross. The electrodes are two parallel uncoated stainless steel plates of 5 cm in diameter and 3.7 cm apart. Electrons were produced by irradiating the cathode with ArF laser (193 nm) photons (Lumonics model 861S). The pulse duration is about 10 ns. A negative high voltage was applied to the cathode. The conduction current induced by electron motion between the electrodes was converted into a transient voltage pulse

across a resistor connecting the anode to ground. The transient voltage was monitored by a storage oscilloscope (HP model 1727A) and photographed for a permanent record. The electron attachment rates are determined by comparing the transient voltages with and without C_3F_8 in various buffer gases as described in earlier papers.^{9,10} The electron drift velocities were determined from the duration of transient pulses and the electrode separation.

The gas pressure in the cell was maintained constant in a slow flow system (flow rate ~ 20 STP cm³/min). The gas pressure was measured by an MKS Baratron manometer. All measurements were done at room temperature. The Ar, N_2 , and CH_4 gases (supplied by MG Scientific) have minimum purities of 99.998%, 99.998%, and 99.99%, respectively. The perfluoropropane (C_3F_8) supplied by Matheson has a minimum purity of 99.0%. Because the C_3F_8 concentrations used in the Ar experiment were usually small, a diluted 3% of C_3F_8 in prepurified Ar (supplied by Matheson) was used so that the partial pressure of C_3F_8 could be measured accurately.

III. RESULTS

A. C_3F_8 -Ar mixture

The electron transient pulses for C_3F_8 -Ar mixtures at $E/N = 3$ Td (1 Td = 10^{-17} V cm²) are shown in Fig. 1, where the pressure of Ar is 380 Torr, and the pressures of

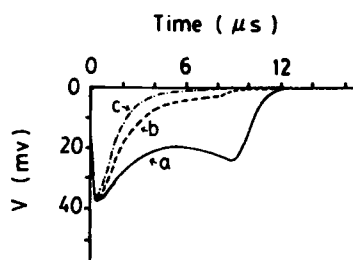


FIG. 1. The transient voltage waveforms produced from the electron motion in 380 Torr of Ar (a) without C_3F_8 , (b) with 0.02 Torr, and (c) with 0.04 Torr of C_3F_8 . The electrons were produced from irradiation of the cathode by ArF laser photons. The E/N was fixed at 3 Td, the electrode spacing was 3.7 cm, and the external resistor was 2 k Ω .

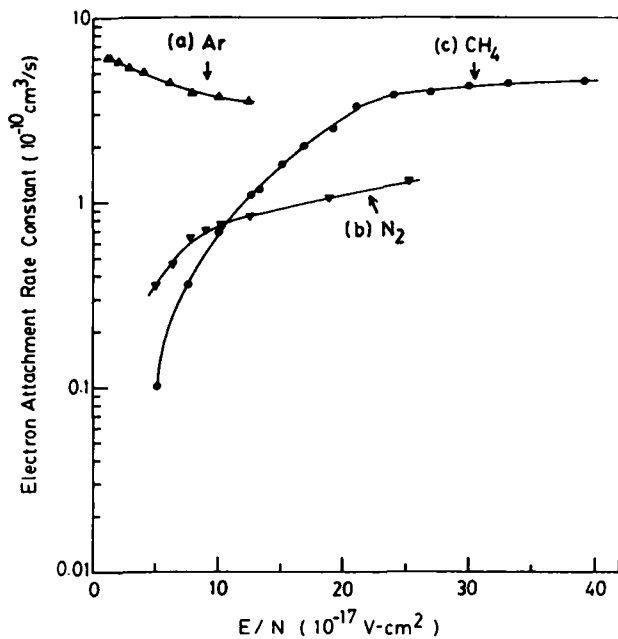


FIG. 2. Electron attachment rate constants of C_3F_8 in the buffer gases of (a) 380 Torr of Ar, (b) 320 Torr of N_2 , and (c) 250 Torr of CH_4 .

C_3F_8 are (a) 0, (b), 0.02, and (c) 0.04 Torr. As shown in the figure, the electron pulses are shortened when small amounts of C_3F_8 are added to Ar. The shortening is caused by the electron attachment of C_3F_8 . The electron attachment rate v_a for a C_3F_8 concentration is obtained from the ratio of transient voltages with and without C_3F_8 in Ar as a function of time (see previous papers^{9,10} for detail). The electron attachment rate constant k_a is determined by $v_a/[C_3F_8]$. We find that the k_a values decrease with increasing $[C_3F_8]/[Ar]$, as reported earlier by Hunter and Christophorou.⁵ This is likely caused by the effect of C_3F_8 on the electron energy distribution in Ar, similar to the case^{10,11} of H_2O in Ar. The attachment rate constant of C_3F_8 is the value of extrapolating $v_a/[C_3F_8]$ to $[C_3F_8] = 0$, for which the electron energy distribution is associated with pure Ar. The results of k_a at various E/N are shown in Fig. 2(a), where the Ar pressure is about 380 Torr. The experimental uncertainty is estimated to be $\pm 20\%$ of the given value. [Figs. 2(b) and 2(c) show the electron attachment constant for the C_3F_8 - N_2 and C_3F_8 - CH_4 mixtures as discussed in Sec. III B and Sec. III C.]

The attachment rate constant is about $6 \times 10^{-10} \text{ cm}^3/\text{s}$ at $E/N = 1.2 \text{ Td}$, and decreases with increasing E/N . A gas mixture with the nature of this E/N dependence will take a

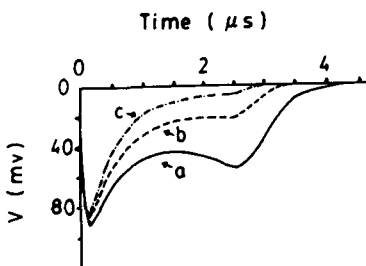


FIG. 3. The transient voltage waveforms produced from the electron motion in 320 Torr of N_2 (a) without C_3F_8 , (b) with 0.2 Torr, and (c) with 0.8 Torr of C_3F_8 . The E/N was fixed at 8.9 Td. The electrode spacing was 3.7 cm, and the external resistor was 510Ω .

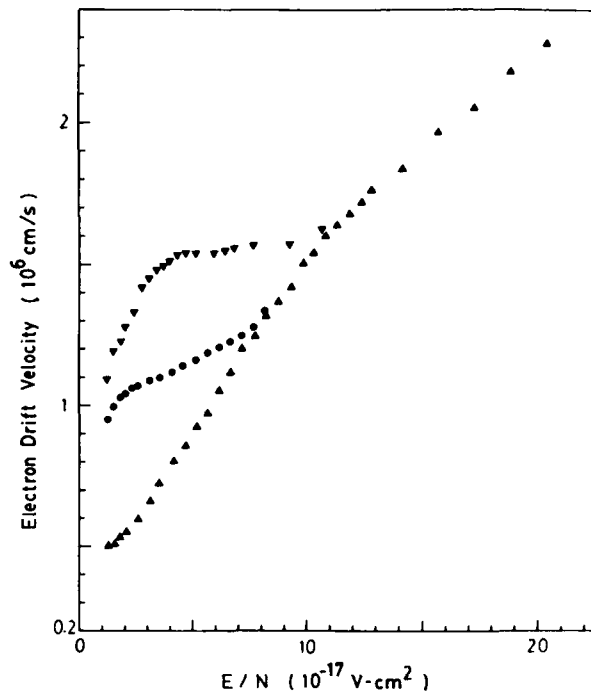


FIG. 4. The electron drift velocities in the C_3F_8 - N_2 mixture as a function of E/N . The $[C_3F_8]/[N_2]$ ratios are 0 (\blacktriangle), 0.63% (\bullet), and 1.5% (\blacktriangledown).

long time to open a discharge switch.^{1,2} Therefore, for the case of low C_3F_8 concentration the C_3F_8 -Ar mixture is not desirable for the application of diffuse-discharge opening switches. However, in a practical switching device, the C_3F_8 concentration can be so high that the C_3F_8 -Ar mixture is useful for the switching application as stated in Ref. 5.

The electron drift velocity W is measured in this experiment, which is equal to the ratio of the electrode spacing to the electron drift time. Because of the fast decay of conduction pulse at high $[C_3F_8]$ (see Fig. 1), the electron drift velocity is only measurable at low C_3F_8 concentration ($< 0.02\%$) in Ar. The measured electron drift velocity increases substantially when a small amount of C_3F_8 is added to Ar. At high E/N , the electron drift velocity for the C_3F_8 -Ar mixture merges with the value for pure Ar. Our observation for the electron drift velocity of the C_3F_8 mixture is consistent with the measurements of Christophorou *et al.*^{4,6,7}

B. C_3F_8 - N_2 mixture

The electron conduction pulses for 0, 0.2, and 0.8 Torr of C_3F_8 in 320 Torr of N_2 are shown in Figs. 3(a), 3(b), and 3(c), respectively, where the E/N is fixed at 8.9 Td. Again, the shortening of electron pulses in Fig. 3 is due to the electron attachment to C_3F_8 . The electron attachment rate constants of C_3F_8 in N_2 are slightly dependent on the contents of C_3F_8 as reported earlier by Hunter and Christophorou.⁵ The k_a values measured at $[C_3F_8] \rightarrow 0$ are shown in Fig. 2(b) as a function of E/N from 5 to 25 Td. The attachment rate constants of C_3F_8 in N_2 increase with increasing E/N . This characteristic is desirable for the application of a diffuse-discharge opening switch.

The electron drift velocities measured at various E/N as various $[C_3F_8]/[N_2]$ ratios are shown in Fig. 4. When a small

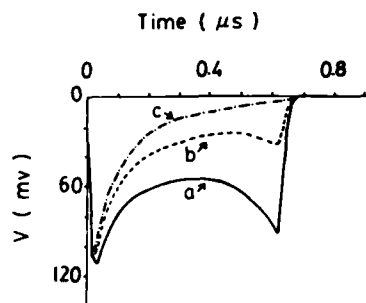


FIG. 5. The transient voltage waveforms produced from the electron motion in 250 Torr of CH_4 (a) without C_3F_8 , (b) with 0.15 Torr, and (c) with 1.0 Torr of C_3F_8 . The E/N was fixed at 39 Td. The electrode spacing was 3.7 cm, and the external resistor was 51Ω .

small amount of C_3F_8 is added to N_2 , the drift velocity increases at low E/N but remains unchanged at high E/N , which is similar to the characteristic observed in the C_3F_8 -Ar mixture.⁴ The electron drift velocity shows a small bump when more C_3F_8 is added (see Fig. 4). The increase of electron drift velocity due to the addition of C_3F_8 to N_2 is also a characteristic desirable for the design of diffuse-discharge opening switches.

C. C_3F_8 - CH_4 mixture

The electron conduction pulses with 0, 0.15, and 1.0 Torr of C_3F_8 in 250 Torr of CH_4 are shown in Figs. 5(a), 5(b), and 5(c), respectively, where the E/N is fixed at 39 Td. Since the electron drift velocity in CH_4 is much higher than that in

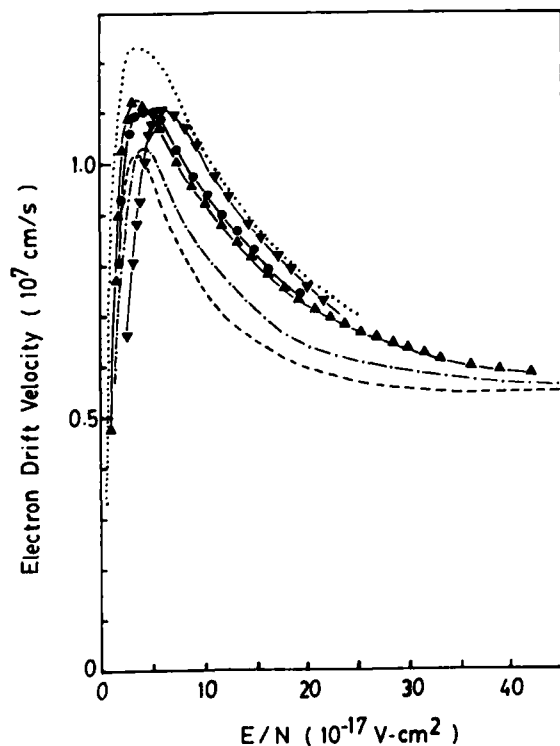


FIG. 6. The electron drift velocities in the C_3F_8 - CH_4 mixture as a function of E/N . The $[\text{C}_3\text{F}_8]/[\text{CH}_4]$ ratios are 0 (\blacktriangle), 0.48% (\bullet), and 1.79% (\blacktriangledown). The data from Ref. 8 with $[\text{C}_3\text{F}_8]/[\text{CH}_4] = 0.5\%$ (---) and 2% (-.-), and from Ref. 12 with pure CH_4 (···) are plotted for comparison.

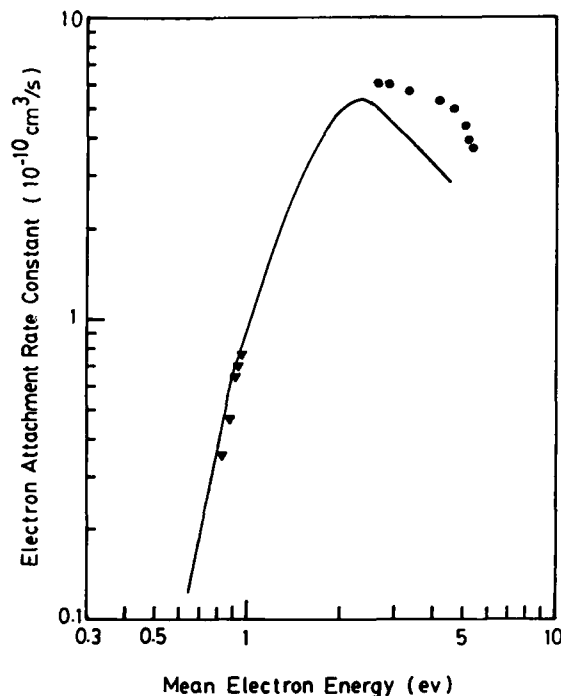


FIG. 7. Electron attachment rate constants of C_3F_8 in Ar (\bullet) and N_2 (\blacktriangledown) as a function of mean electron energy. The data from Ref. 5 (solid line) are plotted for comparison.

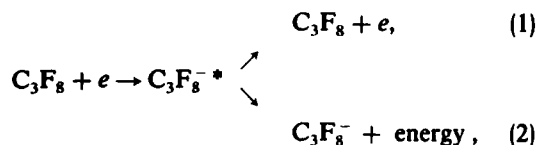
Ar and N_2 , the pulse duration observed here is relatively short. The attachment rate constants of C_3F_8 in CH_4 measured at various E/N are shown in Fig. 2(c). The k_a values increase by a factor of about 40 from $E/N = 5$ to 39 Td as shown in Fig. 2(c). The dependence of this electron attachment rate constant on E/N is very desirable for the application of diffuse-discharge opening switches.

The electron drift velocities for the C_3F_8 - CH_4 mixture measured at various $[\text{C}_3\text{F}_8]/[\text{CH}_4]$ ratios as a function of E/N are shown in Fig. 6. The experimental uncertainty for the electron drift velocity is estimated to be within $\pm 10\%$ of the given value, which is mainly caused by the time measurements. The uncertainty for the time measurement in the beginning or the end of a pulse is about 20 ns. This causes an uncertainty for the electron drift velocity of about 7%. The measurements of Hunter *et al.*⁸ with $[\text{C}_3\text{F}_8]/[\text{CH}_4] = 0.5\%$ and 2%, and the measurement of Hurst *et al.*¹² with pure CH_4 are also plotted in Fig. 6 for comparison. Our measured values are between those two previous results and are consistent within experimental uncertainties. The electron drift velocity is affected by the addition of C_3F_8 to CH_4 . The electron drift velocities have maxima in the E/N region of 5–10 Td. The peak position shifts toward the high E/N side when the C_3F_8 concentration increases. Comparing with the C_3F_8 -Ar and C_3F_8 - N_2 mixtures, the electron drift velocity in the C_3F_8 - CH_4 mixture is less sensitive to the contents of C_3F_8 . The electron drift velocity for the C_3F_8 - CH_4 mixture is very high ($\sim 1.1 \times 10^7$ cm/s) at moderate E/N (5–7 Td). Although the electron drift velocity decreases with increasing E/N , its value at $E/N = 40$ Td is still quite large (6×10^6 cm/s). This characteristic is very desirable for designing diffuse-discharge opening switches.

IV. DISCUSSION AND CONCLUSION

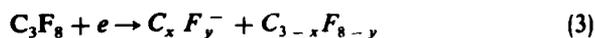
For a comparison of our measurements with the published data, the attachment rate constants of C_3F_8 in N_2 and Ar are plotted in Fig. 7 as a function of the mean electron energy $\langle \epsilon \rangle$, where $[Ar] = 380$ Torr and $[N_2] = 320$ Torr. The mean electron energies in N_2 and Ar at each E/N are obtained from Ref. 5. The data of Hunter and Christophorou⁵ are plotted as the solid line in Fig. 7, where the buffer gas pressure (N_2 or Ar) is 1000 Torr.

Christophorou's group^{5,13} have observed that the electron attachment rate constant of C_3F_8 depends on the total pressure for pressures larger than 1000 Torr. This pressure dependence was attributed to the processes⁵



where an electron initially captured by C_3F_8 forms a temporary parent negative ion $C_3F_8^{-*}$. The parent negative ion will either autoionize or be stabilized by collision with the buffer gas. So the higher the buffer gas pressure is, the larger the electron attachment rate will be.

In our experiment, we have measured the electron attachment rate constants as a function of the buffer gas pressure for pressures less than 1 atmosphere. The measured electron attachment rate constants are not sensitive to the buffer gas pressure. For instance, for the C_3F_8 -Ar gas mixture at $E/N = 2.2$ Td ($\langle \epsilon \rangle = 3.55$ eV⁵), the electron attachment rate constants increase less than 10% when the Ar pressures increase from 270 to 760 Torr. The relative less dependence of the electron attachment rate constants on the buffer gas pressure in this experiment may be due to the high mean electron energy we studied (0.8–6 eV) in which the dissociative electron attachment process is important. The dissociative electron attachment processes of C_3F_8 are given as¹⁴



where $x = 0-3$ and $y = 0, 3, 5, 7$. The lowest appearance onset energy¹⁴ for these processes is 1.1 ± 0.1 eV that produces $C_2F_3^-$. The electron attachment due to this dissociative attachment process will show pressure independence. Our observation that the measured electron attachment rate constants are not sensitive to the buffer pressure indicates

that this dissociative electron attachment may be a major process occurring at high E/N .

In summary, we have employed a relatively new method to measure the electron attachment rate constants of C_3F_8 in the buffer gases of Ar, N_2 , and CH_4 . Our measured k_a values as a function of $\langle \epsilon \rangle$ are consistent with the published data.⁵ In this study, we find that the C_3F_8 - CH_4 mixture has a high electron drift velocity and its electron attachment rate constant increases with increasing E/N . These characteristics are desirable for the application of diffuse discharge opening switches.

ACKNOWLEDGMENT

The authors wish to thank Dr. E. R. Manzanares, Dr. J. B. Nee, Dr. M. Suto, and Dr. D. Taylor in our laboratory, and Professor M. A. Fineman at San Diego State University for useful suggestions and discussion. This work is supported by the Air Force Office of Scientific Research, Air Force Office Systems Command, USAF, under Grant No. AFOSR-82-0314.

¹K. H. Schoenbach, G. Schaefer, M. Kristiansen, L. L. Hatfield and A. H. Guenther, IEEE Trans. Plasma Sci., PS-10, 9246 (1982).

²K. H. Schoenbach, G. Schaefer, M. Kristiansen, L. L. Hatfield, and A. H. Guenther, in *Electrical Breakdown and Discharges in Gases*, Part B, edited by E. E. Kunhardt and L. H. Luessen (Plenum, New York, 1983), p. 415.

³J. K. Burton, D. Conte, R. D. Ford, W. H. Lupton, V. E. Scherrer, and I. M. Vitkovitsky, in *Digest of Technical Papers*, 2nd IEEE International Pulse Power Conference, Lubbock, Texas, edited by A. Guenther and M. Kristiansen (IEEE, New York, 1979), p. 284.

⁴L. G. Christophorou, S. R. Hunter, J. G. Carter, and R. A. Mathis, Appl. Phys. Lett. 41, 147 (1982).

⁵S. R. Hunter and L. G. Christophorou, J. Chem. Phys. 80, 6150 (1984).

⁶L. G. Christophorou and S. R. Hunter, *Electron-Molecule Interactions and Their Application*, Vol. 2, edited by L. G. Christophorou (Academic, Orlando, 1984), p. 317.

⁷L. G. Christophorou, S. R. Hunter, J. G. Carter, S. M. Spyrou, and V. K. Lakdawala, *Proceeding of the 4th IEEE International Pulsed Power Conference*, edited by T. H. Martin and M. F. Rose (Texas Tech., Lubbock, TX, 1983), p. 702.

⁸S. R. Hunter, J. G. Carter, L. G. Christophorou, and V. K. Lakawala, *Gaseous Dielectric IV*, edited by L. G. Christophorou and M. O. Pace (Pergamon, New York, 1984), p. 224.

⁹L. C. Lee and F. Li, J. Appl. Phys. 56, 3169 (1984).

¹⁰W. C. Wang and L. C. Lee, J. Appl. Phys. 57, 4360 (1985).

¹¹G. S. Hurst, L. B. O'Kelly, and T. E. Bortner, Phys. Rev. 123, 1715 (1961).

¹²G. S. Hurst, J. A. Stockdale, and L. B. O'Kelly, J. Chem. Phys. 38, 2572 (1963).

¹³S. R. Hunter, L. G. Christophorou, D. R. James, and R. A. Mathis, *Gaseous Dielectrics III*, edited by L. G. Christophorou (Pergamon, New York, 1982), p. 7.

¹⁴S. M. Spyrou, I. Sauters, and L. G. Christophorou, J. Chem. Phys. 78, 7200 (1983).

END

FILMED

1-86

DTIC